CP Aeronautics

With our powers combined™

CP-01 Planeteer ©

Response to 2009/2010 AIAA Foundation Undergraduate Team Aircraft Design Competition
Presented by Virginia Polytechnic Institute and State University

TEAM CP AERONAUTICS ©

Brian Lancaster
Team Leader and Systems
AIAA No. 300963

Nathaniel Lynch
Performance
AIAA No. 292913

Stacy Critchfield
Stability and Control
AIAA No. 416045

TC Montague
CAD
AIAA No. 289271

Joseph Feerst
Weights and Structures
AIAA No. 412830

Andrew Olson
Structures and Biofuels
AIAA No. 415233

Ryan Holcombe
Aerodynamics
AIAA No. 288390

Thomas Steva
Advanced Tech and Cost
AIAA No. 281938

Dr. William Mason
Project Advisor
AIAA No. 11141

Dr. Mayuresh Patil
AIAA Advisor
AIAA No. 144995

Executive Summary

CP Aeronautics is pleased to respond to the American Institute of Aeronautics and Astronautics (AIAA) Undergraduate Team Aircraft Design RFP it received on September 30, 2009. It calls for the development of an alternative fuels and environmentally friendly aircraft system for the year 2020. The CP-01 Planeteer meets the RFP requirement for a 25% improvement in lift-to-drag ratio over modern mid-sized transport aircraft and improvements to the environment in terms of carbon footprint, emissions, and noise. This 737NG / A320 replacement aircraft will have the range capability of at least 3500 nm while reducing noise and environmental emissions and maintaining low fuel consumption. The RFP's goal is to achieve a long range cruising speed of Mach 0.8. It has a balanced field length (BFL) of 8200 feet and a maximum approach speed of 140 knots. It is also required to have an initial cruising altitude of 35,000 feet and a maximum operating ceiling of 41,000 feet. The designed aircraft will meet all Federal Aviation Regulations (FAR). The CP Aeronautics concept is a strut-braced wing airplane, which has been used on small and military aircraft but has not been applied to the commercial airliner industry. The weight and aerodynamic characteristics of a strut-braced wing model were compared to those of existing and proposed wing configurations, but the strut-braced design is superior. CP Aeronautics employs advanced technologies throughout the design to ensure that the design remains competitive in the constantly changing airline industry. CP Aeronautics presents the CP-01 Planeteer (plan-e-teer).

CP Aeronautics

With our powers combined™

CP-01 Planeteer

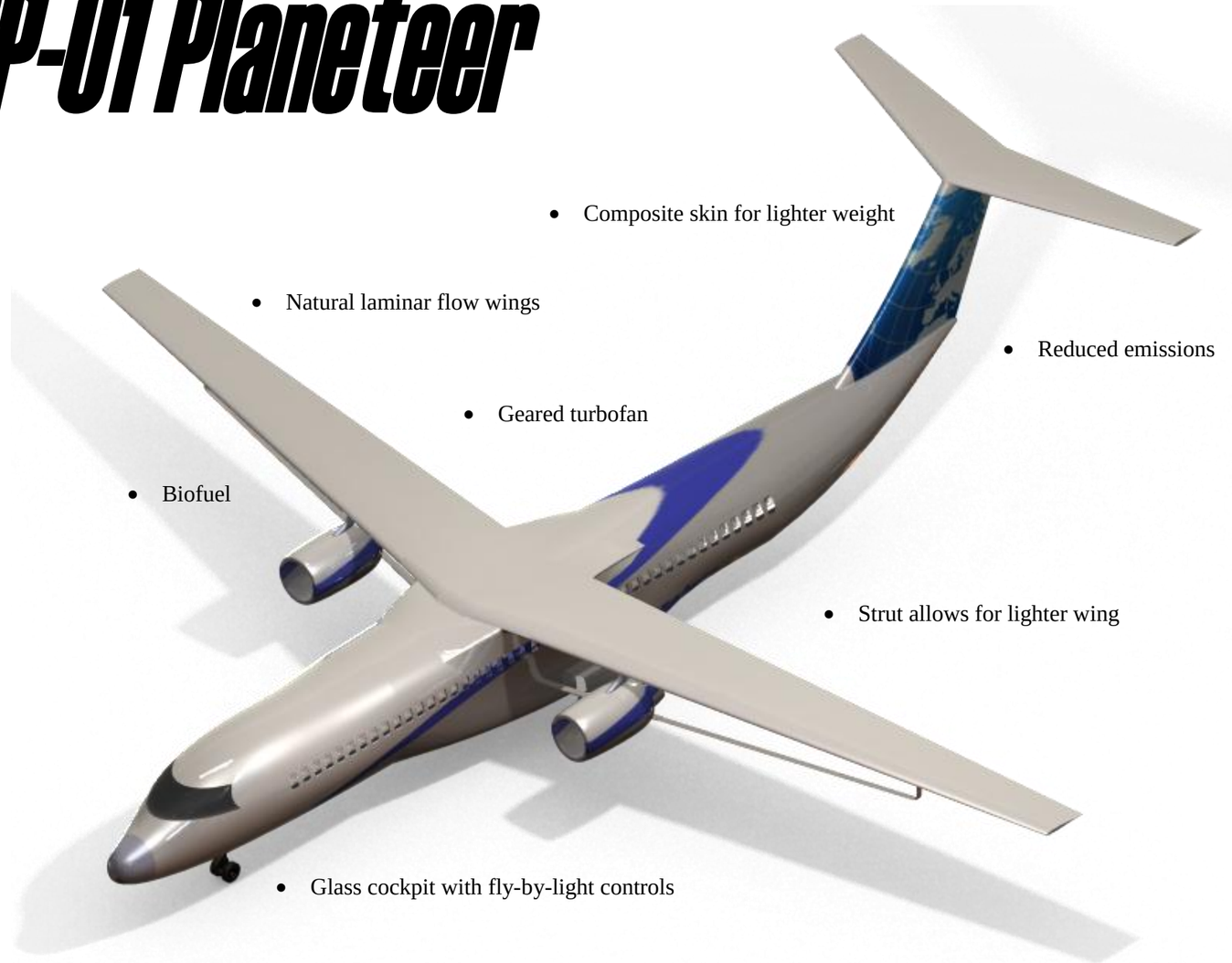

- Composite skin for lighter weight
- Natural laminar flow wings
- Reduced emissions
- Geared turbofan
- Biofuel
- Strut allows for lighter wing
- Glass cockpit with fly-by-light controls

CP-01 Selected Details

Maximum Takeoff Gross Weight	131,381 lbs
Maximum Fuel	30,966 lbs
Maximum Payload	38400 lbs
Passenger Capacity	175
Wingspan	50 ft
Overall Length	135 ft
Overall Height	33 ft
Taper Ratio	0.39
1/4 Chord Sweep	16
Aspect Ratio	15.12
Reference Area	1296 ft^2
Mean Aerodynamic Chord	9.92 ft
Fuel Efficiency (1200 nm mission)	131 pounds per seat
FAA Airport Type Code	C-IV
Thrust Loading	0.25
Wing Loading	95 lbs/ft^2
L/D_{cruise}	26.1
Takeoff Length	4800 ft
Max Designed Range	4,800 ft
Long Range Cruise Speed	Mach 0.8

Table of Contents

Index of Figures

Index of Tables

Nomenclature

AR – Aspect Ratio
b – Wing Span
c – Chord (ft)
Cacq – Acquisition Cost
CD0 – Coefficient of Profile Drag
CDi – Coefficient of Induced Drag
CD – Coefficient of Drag
CDtrim – Coefficient of Trim Drag
CDw – Coefficient of Wave Drag
CLmax – Maximum Coefficient of Lift
CLp – Lift Coefficient due to Pitch
CLr – Lift Coefficient due to Rudder
CLα – Lift Coefficient due to Angle of Attack
CLβ – Lift Coefficient due to Sideslip
CLδr – Lift Coefficient with Rudder Deflection
CMq – Moment Coefficient due to Pitch
CMα – Moment Coefficient due to Angle of Attack
CNavail – Yawing Moment Available
CNp – Yawing Coefficient due to Pitch
CNr – Yawing Coefficient due to rudder
CNrequired – Yawing Moment Required
CNβ – Yawing Coefficient due to Sideslip
CNδr – Yawing Coefficient due to Rudder Deflection
Copsdir – Indirect Operating Costs
e – Oswald's efficiency factor
g – Gravity (ft/s2)
kA – Airfoil Technology Factor
L/D – Lift to Drag Ratio
lto – Take-off Field Length (ft)
M – Mach Number
Mcrit – Critical Mach Number
MDD – Drag Divergence Mach Number
Nyr – Number of Years Aircraft is Operated
Rbl – Total Annual Block Miles Flown (nm)
S – Wing Area (in2)
t/c – Thickness to Chord Ratio
T/W – Thrust to Weight
Tc – Thrust at Cruise (lbs)
To – Thrust at Take-off (lbs)
VA – Approach Velocity (knots)
W – Weight (lbs)
W/S – Wing Loading
Wempty – Empty Weight of Aircraft (lbs)
Wfixed – Fixed Weight (lbs)
Wfuel – Weight of Fuel (lbs)
β – Sideslip angle
δa – Aileron Deflection
δr – Rudder Deflection
Λ – Wing Sweep
ρsl – Density at Sea Level (slug/ft3)
σ – Density Ratio
φ – Flight path angle

1 Introduction

In 2008 airlines spent $61.2 billion on petroleum based jet fuel in the U.S. alone[1]. Despite what may seem like overwhelming costs, aviation fuel consumption is not only an economic concern but an environmental one as well. Aircraft release about 600 million tons of CO_2 each year[1]. This CO_2 has a disproportionately greater impact as a greenhouse gas than most CO_2 emissions as it is released directly into the upper atmosphere[1].

In light of the effects of petroleum-based fuels on our environment there is a need both for alternative fuels and for environmentally-friendly and more fuel efficient aircraft that can meet our nation's needs. The development of aviation technologies and procedures to improve the energy efficiency are key elements of our long-term national goals for aeronautical research. The goal is to enhance the aircraft and engine efficiencies and optimize aircraft operations to minimize fuel burn, noise, and emissions.

1.1 RFP Analysis

The AIAA Foundation Undergraduate Team Aircraft Competition RFP calls for an aircraft design that could be ready for service in 2020 incorporates new technologies, operational procedures, and alternative fuels. A 25% improvement lift-to-drag ratio will be targeted based on novel configuration utilizing multidiscipline configuration optimization and laminar flow technology. Furthermore, indentifying specific improvements to the environment in terms of carbon footprint, emissions, and noise will be necessary as part of the design study. The design is intended to be a 737NG/A320 replacement aircraft.

The general requirements for the aircraft are representative of the 737NG/A320 class aircraft that the design shall replace. The aircraft must be capable of transporting 175 passengers in one class with a seating pitch of 32" and a seat width of 17.2". The vehicle must be able to carry a payload weight of at least 37,000 lbs with a cargo volume of 1240 ft^3.

The range requirement is that the maximum range must be at least 3500 nm while the nominal range is 1200 nm. It is required that the plane cruise at Mach 0.8. The target cruise altitude is to be 35,000 ft but the aircraft must be able to attain a cruise altitude of at least 41,000 ft. It is also required that the aircraft is capable of landing at speeds less than 140 knots at maximum landing weight. The RFP further states that the aircraft must have a takeoff distance no longer than 8200 ft. It is also desired that the noise level be reduced and overall emissions be cut. Naturally, the designed aircraft must be certifiable to the appropriate FAA regulations.

In addition to the design of a new aircraft an entirely new aircraft system must be analyzed. The RFP requires that ground systems be defined and evaluated to determine the alternative fuel costs. Operation and maintenance costs will be assessed against current in-service aircraft. The design will also be assumed to be operating under the Federal Aviation Administration's (FAA) NextGen initiative. Environmental impact must also be evaluated. These include the carbon footprint of operating, the acquisition of the alternative fuel and changes to the airline infrastructure. Airline impacts to utilize the alternative fuels and additional infrastructure will also need to be assessed.

1.2 Mission Profile

The mission profile derived from the RFP for the 2009-2010 AIAA competition is shown in Figure 1.1.

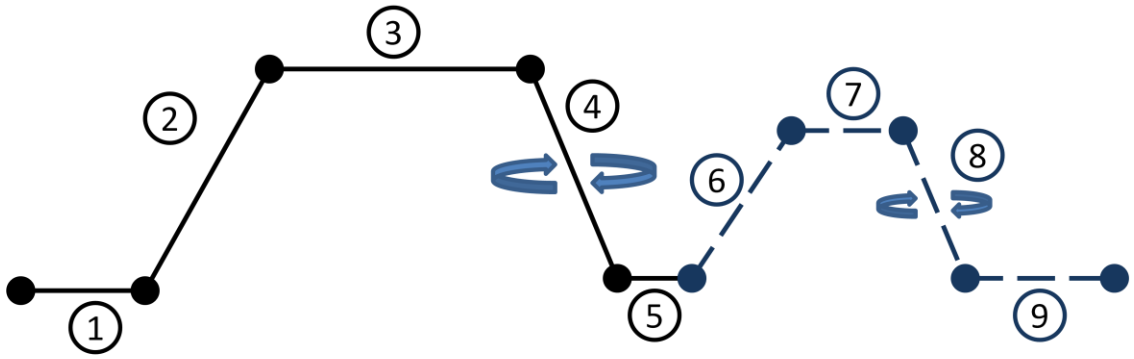

1. Takeoff
2. Climb to 35k ft
3. 2200nmi cruise at 35k ft, M=0.8
4. Loiter 20 minutes at 10k ft
5. Landing / Aborted Landing
6. Climb to 10k ft
7. 200nmi cruise at 10k ft, M=0.8
8. Loiter 20 minutes at 10k ft
9. Landing

Figure 1.1 Mission profile for the 2009/2010 AIAA RFP Design

2 Preferred Concept Evolution

The design process began with each member of the group forming their own ideas and sketches of what kind of aircraft would best meet the RFP requirements. The eight members each submitted their results for group evaluation. Of the eight proposed design concepts only three were chosen. These three designs can be found in the following sections, consisting of a conventional (cantilever) design, a strut-braced wing, and a blended wing body. Analysis of these three designs found that each was capable of fulfilling the RFP.

2.1 Conventional Design

The conventional design closely resembles the existing Boeing 737 and Airbus A320 narrow-body passenger jets it is meant to replace, following the basic configuration for nearly all airliners established by the original Boeing 367-80 prototype. The concept can be seen in Figure 2.1. It includes a low wing, with engines mounted in pods beneath the wing, tricycle landing gear, a conventional tail, and the payload contained in a cylindrical fuselage.

Most of the benefits of this design stem from its ubiquitous use: the design is very well understood, with numerous examples of in-service aircraft to inform the design process. It is also easily accepted by both airlines, passengers, and the regulatory agency representatives responsible for certifying its airworthiness. This design would also integrate easiest with existing infrastructure. Finally, it is well understood that the "tube-and-wing" concept, with a cylindrical fuselage, offers an advantageous pressure vessel design in reducing the weight associated with a pressurized aircraft.

The principle problem with this concept is that it is a legacy design, refined over 50 years, and thus any improvements are likely to be evolutionary and incremental, with little room for the significant aerodynamic improvements called for in the RFP. A table of current conventional wing aircraft can be found in Table 2.1 below.

Table 2.1 Comparator Aircraft[2,3,4]

Model	Year	Passengers	Wingspan (ft)	Length (ft)	Max Mach	Cruise Mach	Max Altitude (ft)	T-O/Landing field length (ft)	Design range (nm)	OWE (lb)	MTOW (lb)	Max payload (lb)
Airbus A320-200	1988	179	111.8	123.3	0.82	0.78	39800	7385 / 4890	3045	92815	169755	41079
Boeing 737-800	1997	189	117.4	129.5	0.82	0.785	41000	6890 / 5400	1990	90710	155500	44700
Bombardier C300	2010+	130	115.1	124.8	0.82	0.78	41000	6240 / 4750	2200	NA	131800	38200

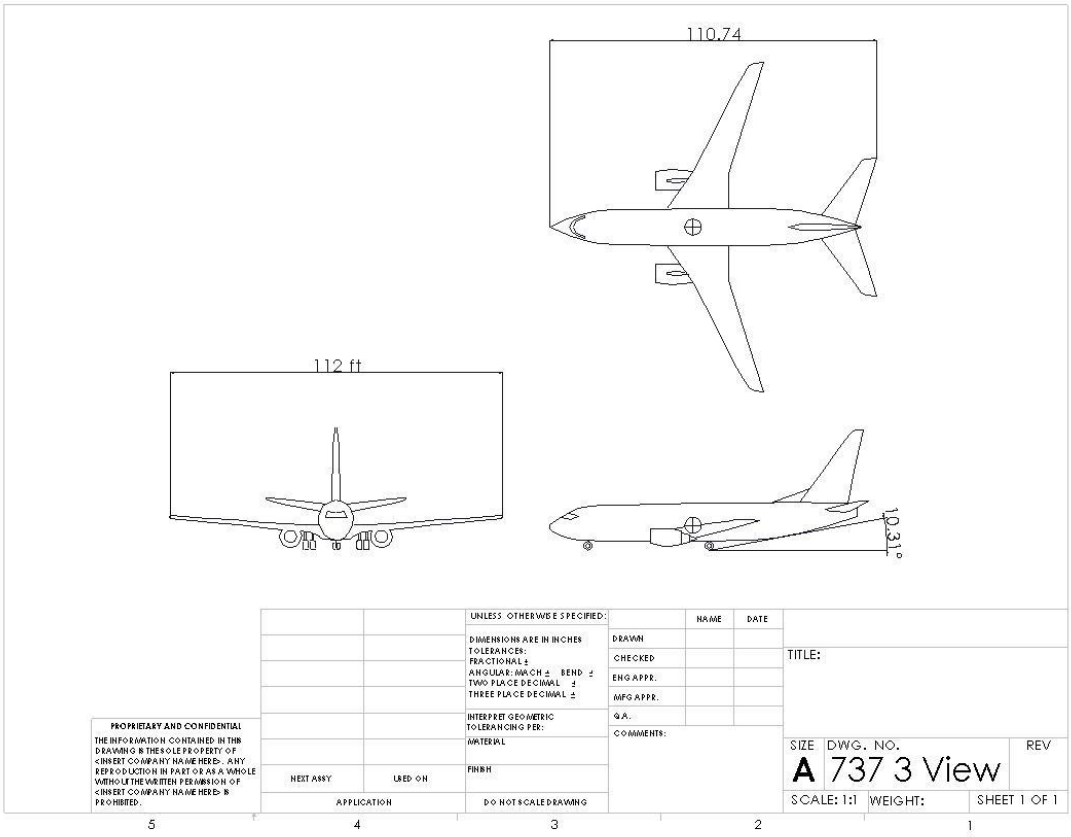

Figure 2.1 Conventional design consideration.

2.2 Blended Wing Body

The blended wing design originates from the desire to have the entire plane act as a lifting surface. This desire leads to design the fuselage to follow the contours of an airfoil, gently morphing into the wing shape[5]. Due to the entire plane being a lifting surface, more lift is generated with less wetted area, and less wing loading. The reduction in loading and weight from less fuel required leads to less structural weight[6].

Another advantage to the blended-wing design is the ability to place the engines on top of the aircraft, resulting in ground noise reduction. Since the entire surface is a wing, the internal volume is extremely large. This is why the blended-wing design is often developed as a potential concept for cargo planes[2].

This design is extremely effective for large aircraft, when the wing can be adapted to be thick enough to hold cargo, acting as a fuselage[5]. The non-cylindrical fuselage makes maintaining cabin pressure difficult. Overcoming this complexity would likely result in extra production costs. The preliminary design concept can be seen in Figure 2.2.

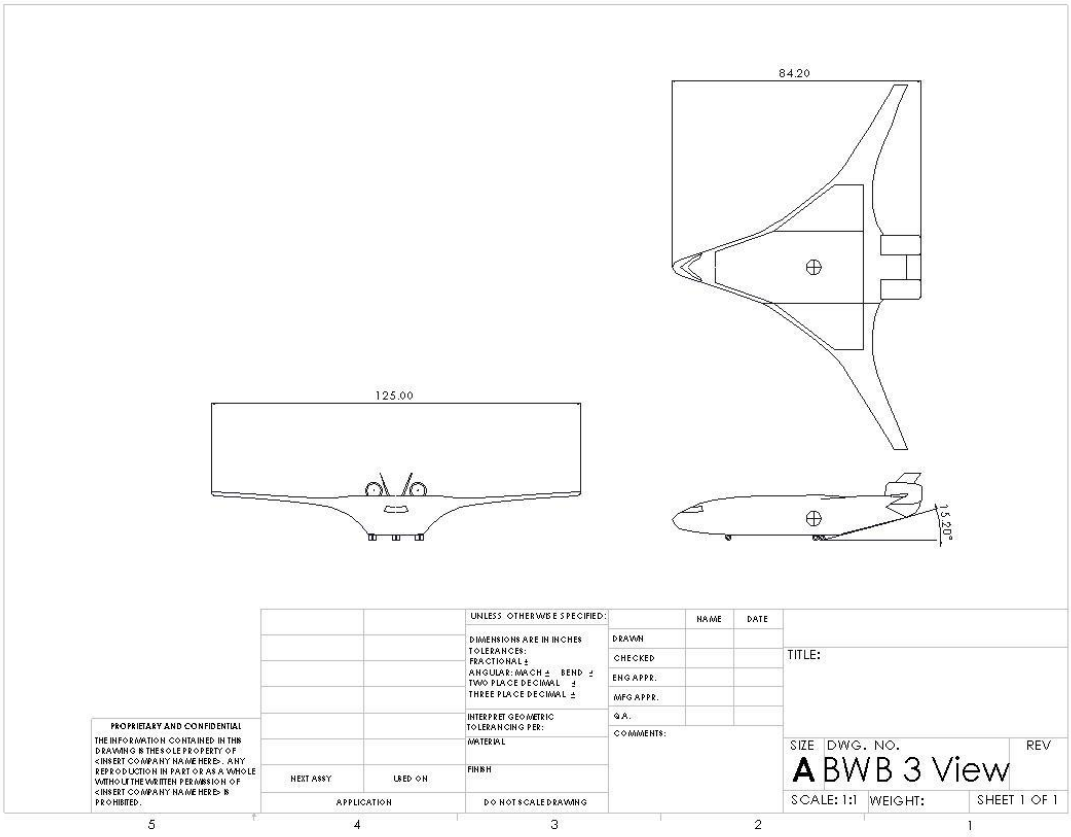

Figure 2.2 Blended Wing Body design.

2.3 Strut-Braced Wing

The third concept investigated by CP Aeronautics is a strut-braced wing design, seen in Figure 2.3. While at first sight it may appear quite similar to a conventional commercial aircraft design with the addition of a strut, it has many significant differences that make it an ideal design choice. First of all, it is important to understand why the strut is implemented and how it affects the rest of the aircraft. The main purpose of the strut is to relieve some of the stress encountered by the wing due to wing loading.

Struts are very efficient in tension. However, when subjected to compression struts are susceptible to buckling. The strut reduces the force carried by the wing when lift is present by transferring part of that load to the strut in tension. With this reduced force on the wing, less skin thickness is required on the wing itself for structural integrity. This reduced skin thickness causes the wing to weigh much less than a conventional wing even when the strut weight is included. Furthermore, the wing sweep, which is dependent upon airfoil thickness, can also be decreased. With smaller airfoil thickness, the critical Mach number location is delayed along chord length. Although

wing sweep delays the critical Mach number; less sweep is necessary to achieve this objective with reduced airfoil thickness[7]. These sources of decreased aircraft weight leave more room available for increasing wing span. With an increase in span and a larger planform area, aspect ratio and aircraft lift coefficient will ultimately increase. Lastly, the strut-braced wing concept allows for alternate fuel locations with cargo weight to spare.

In the current strut-braced wing design, one should notice the high wing. For a strut to be properly implemented into this aircraft design, a high wing is necessary. If the strut were to be introduced to a basic low, dihedral wing, the strut would have not have an effective position to occupy. The strut could be placed on the top of the fuselage, in an inverted manner; however, as mentioned earlier, struts are inefficient when dealing with compression. Another aspect to point out is the vertical member of the strut that connects to the wing. The primary reason for this design feature is to minimize the interference caused between both the strut and wing. Assuming that a vertical member creates little or no lift, the main section of the strut and wing can operate effectively while experiencing minimal aerodynamic interference.

On the topic of interference, the horizontal tail is mounted as a T-tail, or high tail, so that it may encounter clean, undisturbed air flow. If a traditional horizontal tail were used, it would surely encounter the wing wake. The last major feature associated with the strut-braced wing concept is the wide bottom fuselage. The main reason for implementing this design is to provide room for the landing gear. Most conventional commercial aircraft have a rear landing gear system installed in the wing root. However, given a high wing, this is almost impossible. Therefore the base of the fuselage must be wide enough to house the landing gear and maintain stability. Currently this wide base spans almost the full length of the fuselage. The motivation behind this arose from the weight savings influenced by the strut. This added volume may be used for extra cargo space or for alternate storages of fuel.

Like all designs, tradeoffs exist, and there are few pertaining to the strut-braced wing concept to point out. Most aircraft are required to sustain a -2g taxi bump requirement to ensure the wings have a solid connection with the fuselage. This may pose a problem for the strut-braced wing since heavy compression may cause the strut to fail. Still, this remains to be seen and will require extensive calculation to determine the strength of the strut. Also, it is important to note that while the current design will minimize the interference drag encountered between the wing and strut, the overall drag created by aircraft surely increase given its increased wing span and larger wetted area. Lastly, the implementation of the strut will prove challenging during the manufacturing process. The addition of this component will increase the time required to build the aircraft and will increase the need for skilled labor.

Overall, the strut-braced wing design's advantages outweigh its disadvantages and certainly trump those of its competitors. It's unique, yet simple design, demonstrates key objectives emphasized by the project drivers, including increased lift to drag ratio, decreased weight, and reduced fuel consumption. Furthermore, it appears similar to conventional aircraft and is designed for biofuel compatibility which will make it both sustainable and highly marketable. The strut-braced wing concept's overall satisfaction of the RFP and compatibility with project drivers makes this design the optimum choice to correct the issues of current aircraft.

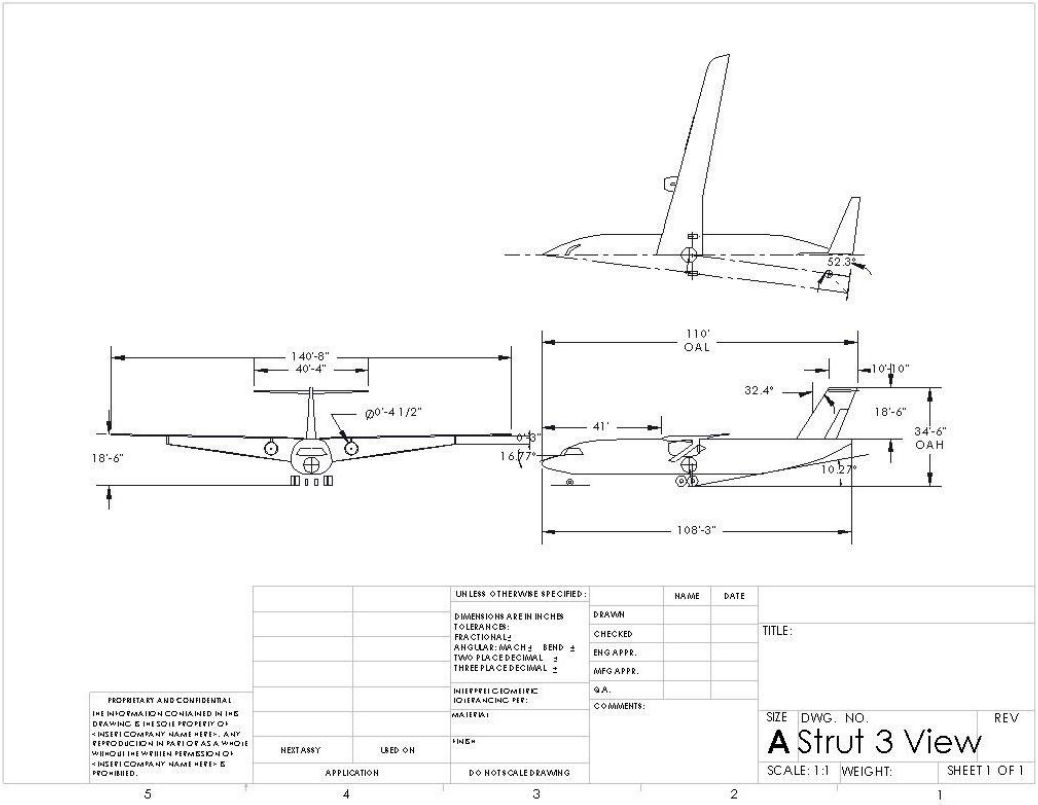

Figure 2.3 Strut-braced wing design.

2.4 Initial Design Sizing

To provide a basis for comparison, the three concepts previously presented were analyzed by estimating the surface area and characteristic length for each major component, which was then fed into a MATLAB implementation of the friction drag code.[54] This code estimates profile drag only, excluding wave drag and interference drag, although it does account for the effects of compressibility on skin friction drag. This drag estimate was then used to estimate the corresponding maximum lift over drag possible for the concept, to help distinguish between the concepts aerodynamically, using the following equation:

$$\left(\frac{L}{D}\right)_{max} = \frac{1}{2}\sqrt{\frac{\pi ARe}{C_{D,0}}} \quad (2.1)$$

The results of this analysis are presented in Table 2.2 and clearly show the strut-braced wing concept has the highest potential L/D_{max} of the three concepts we considered.

Table 2.2 Performance data for the three concepts

Concept	C_{D0}	L/D_{max}
Conventional	0.01655	**20.7**
Strut-Braced Wing	0.01981	**25.8**
Blended Wing Body	0.01027	**21.7**

2.5 Initial Design Weights

These initial estimates were made using Raymer's approach described in his Chapter 3[8]. This method requires that the initial $(L/D)_{max}$ for each aircraft be known and an estimated weight fraction for each segment in the mission profile. These values are provided to us from the concept sketches and analysis in the previous section and Raymer's text. To begin the analysis, the design "Takeoff gross weight" (W_0) will be needed to be defined:

$$W_0 = W_{crew} + W_{payload} + W_{fuel} + W_{empty} \quad (2.2)$$

The crew, payload, and estimated system weights are constant throughout the analysis, so those values will be:

$W_{crew} = 1{,}400\ lbs$ (7 crew members at 200 lbs each)

$W_{payload} = 37{,}000\ lbs$ (The payload required by the RFP)

The sum of these weights will be known as W_{fixed}.

Raymer provides weight fractions for takeoff, climb, and landing and those values will be (for certain segments of the mission profile):

Table 2.3 Weight fractions given from Raymer's text for certain sections of the mission segment

	Weight Fraction
Takeoff	0.970
Climb	0.985
Landing	0.995

To find the weight fractions of the cruise and loiter segments, the Breguet range equation is rearranged for cruise and loiter:

$$\frac{W_{cruise_{final}}}{W_{cruise_{initial}}} = e^{-\left(\frac{R*C}{V*\left(\frac{L}{D}\right)}\right)} \tag{2.3}$$

Where:

R: Range of the cruise in feet

V: Velocity of the cruise in ft/s

(L/D): Lift over drag of the cruise

C: Specific fuel consumption per second at that altitude and Mach number

For the Loiter segments in the mission profile, the Weight fractions are found by:

$$\frac{W_{loiter_{final}}}{W_{loiter_{initial}}} = e^{-\left(\frac{E*C}{\left(\frac{L}{D}\right)_{max}}\right)} \tag{2.4}$$

Where

E: Loiter time in seconds

The concept sketches can only provide an estimated $(L/D)_{max}$ for each concept, while equation 2.1 requires the (L/D) for cruise. Raymer suggests that 86.6% of $(L/D)_{max}$ be used for the cruise weight fraction calculations and will be used for this analysis. A SFC at cruise of 0.627 per hour was used, corresponding to the CFM56-7B24 turbofan engine, currently used on most 737-800s[9].

All the weight fractions for each segment are multiplied together to form a complete mission weight fraction (W_X/W_0) for each concept aircraft. The only weight lost during flight will be due to fuel. A typical 6% fuel reserve will be applied for each design. The total fuel fraction for each concept will be:

$$W_f/W_0 = 1.06(1 - W_x/W_0) \tag{2.5}$$

This leaves only the empty weight fraction to be found. The iterative method described in Raymer will be used for civil transport jets and an initial guess for W_0 will be 100,000 lbs. The calculated mission and fuel weight fractions for each concept aircraft were found to be:

Table 2.4 Weight mission and fuel fraction using Raymer's method for each concept**.**

	Conventional	Strut-Braced	BWB
$(L/D)_{max}$	20.7	25.8	21.7
W_x/W_0	0.7602	0.7914	0.7674
W_f/W_0	0.2542	0.2211	0.2466

A Matlab code was written to compute the weight estimates for each concept aircraft using Raymer's method. The results from the code and data retrieved for comparative aircraft are provided in Table 2.5:

Table 2.5 Weight estimates using Raymer's method for each concept, and comparative aircraft**.**

	Conventional	Strut-Braced	BWB	737-800 (2,200 nmi range)	A320 (2,200 nmi range)
$(L/D)_{max}$	20.7	25.8	21.7	N/A	N/A
W_e (lbs)	77,141	69,362	75,208	~91,300	~93,920
W_f (lbs)	39,372	30,588	37,179	~41,700	~37,080
W_p (lbs)	37,000	37,000	37,000	~37,000	~37,000
W_e/W_0	0.4980	0.5014	0.4988	~0.5371	~0.5590
W_0 (lbs)	154,913	138,350	150,787	~170,000	~168,000

This table shows each concept's takeoff weight, empty weight, and fuel weight. These estimates are compared to the current 737-800 and A320[14,15]. As the table shows, only one concept has lowered fuel weight compared to the 737-800 and A320 for a 2,200 nautical mile range. From these results, the Strut-Braced wing concept would be the best choice since its lowered fuel weight would be advantageous for an alternate fuel aircraft. Less fuel means lower costs per flight and lowered possible emissions made by the aircraft per mission. A summary of the results are shown in Figure 2.4.

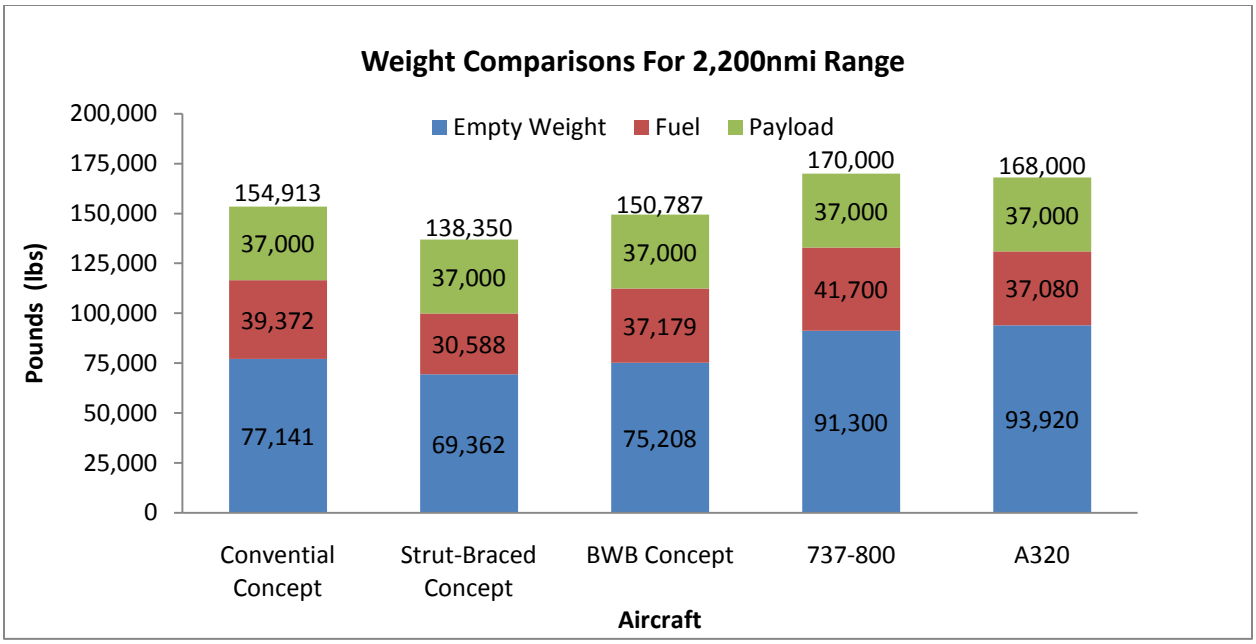

Figure 2.4 Weight comparisons for 3500nmi range.

2.6 Concept Selection

The final design was chosen through the use of a weighting system based on the importance of each concept's characteristics. Every team member was polled on what characteristics of an aircraft's design are essential to determining the best design to fit the requirements set forth by the RFP. The common characteristics were chosen and each was given a weight of importance based on the individual characteristic's role in the overall aircraft design and its ability to meet the RFP. Each concept was then given a score from one to five, with one being the worst and five being the best, for each characteristic. Finally, these scores were multiplied by their respective weights and summed to determine the winner.

Aircraft characteristics given the highest weights were those which would affect the design's ability to meet the requirements of the RFP the greatest. Characteristics like aircraft weight, fuel burn, achievable lift over drag ratio, and ability to fit within the current industry infrastructure play a large role in the aircraft's ability to meet the RFP's fuel saving requirements without drastic changes to the entire industry's system. Characteristics with lower weights are those which drive the aircraft design but don't significantly affect the design's ability to meet the RFP.

The conventional concept was used as a baseline, and thus received a "3" in every category, with the other concepts being graded relative to the conventional design.

Table 2.6 Decision matrix. (highest score is best)

		Conventional	Strut	BWB
	WEIGHTS	SCORE	SCORE	SCORE
Weight	4	3	4	3
Fuel Burn	4	3	5	3
Lift over Drag (achievable)	4	3	4	3.5
Infrastructure	3	3	2.5	2.5
Internal Volume	2	3	3	5
Manufacturing	2	3	3	2
Marketability	1	3	2	1
Noise	1	3	3	5
Ability to Meet FAA Regs	1	3	3	2
	Totals	66	77.5	65.5

After careful consideration using the decision matrix, CP Aeronautics concluded that the best solution to meet and exceed the RFP is the strut-braced wing design. The final 3-view drawing can be seen in Figure 2.6.

2.7 Refined Sizing

With the strut-braced wing concept chosen, the methods proposed by Loftin [47]were used to more accurately size the wing and engine sizes. The engine deck used by Gundlach[25] was used for the decrease of thrust with altitude.

The design point resulting from this constraint analysis is summarized in **Error! Reference source not found.**. The feasible design space is above and to the left of the constraint lines plotted.

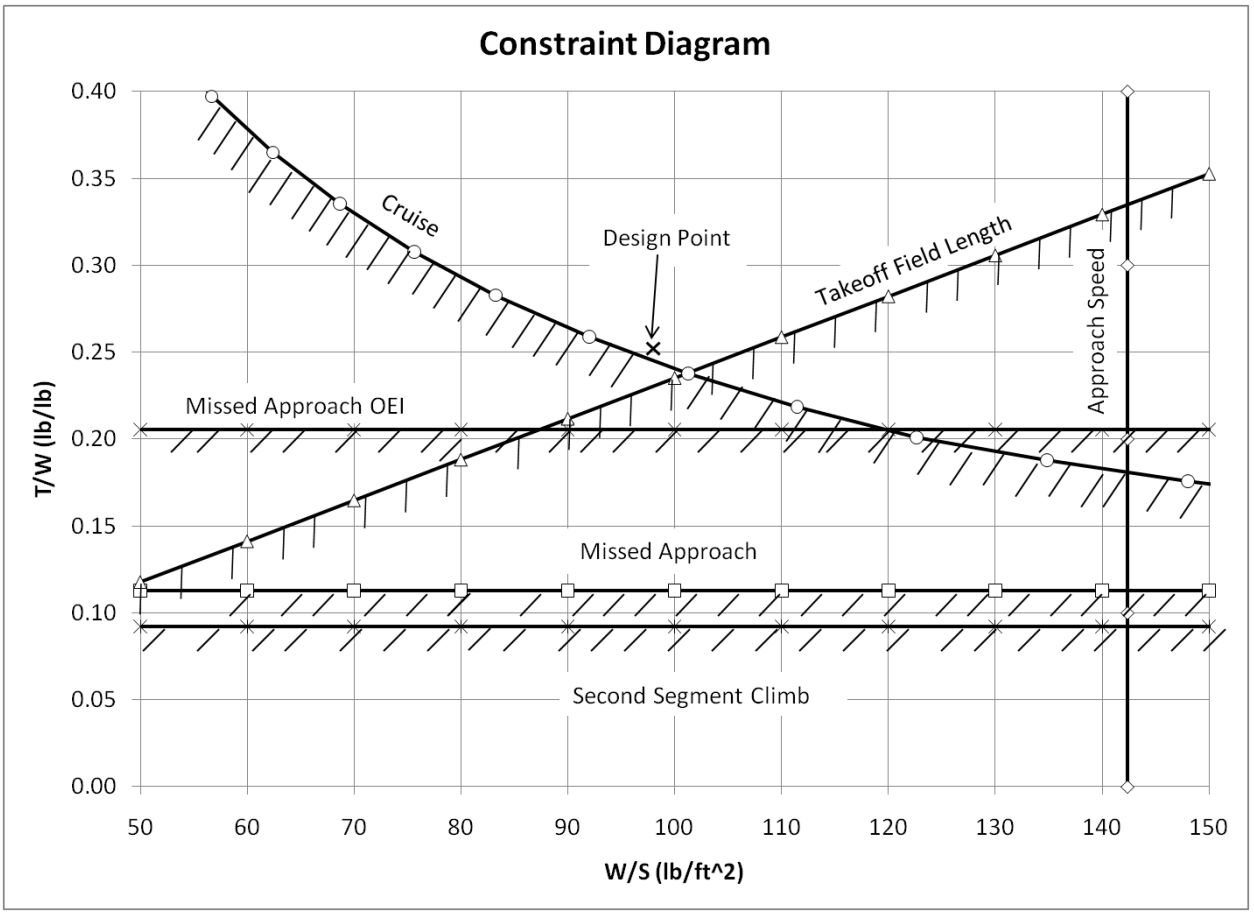

Figure 2.5 Planeteer strut-braced wing constraint diagram.

The basic design parameters used to calculate these constraints are summarized in Table 2.7. A Bypass Ratio of 11 may be considered typical for a modern or near-future high-bypass turbofan that would be used for superior efficiency. This $C_{L,max,clean}$ is achievable using our selected airfoil.

Table 2.7 Summary of constraint diagram design variables.

Variable	Value	Variable	Value
V_A	140 knots	$C_{L,max}$ (with Fowler flaps)	3.29
Takeoff distance	8200 ft	Bypass Ratio	11
Cruise Mach	0.8	Aspect Ratio	15.1
$C_{L,max,clean}$	2.1	Oswald efficiency factor, e	0.95

The wing loading is currently somewhat low, but this provides a growth margin during development, and more importantly, leaves growth potential for future variants with just a higher gross takeoff weight or a fuselage

stretch. With this wing area specified, and the general planform already selected, the design wing can be specified in greater detail, and then analyzed aerodynamically to confirm the required performance.

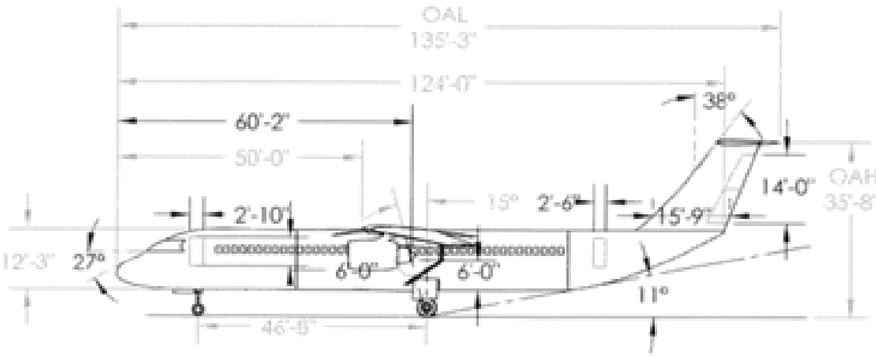

SIDE ELEVATION

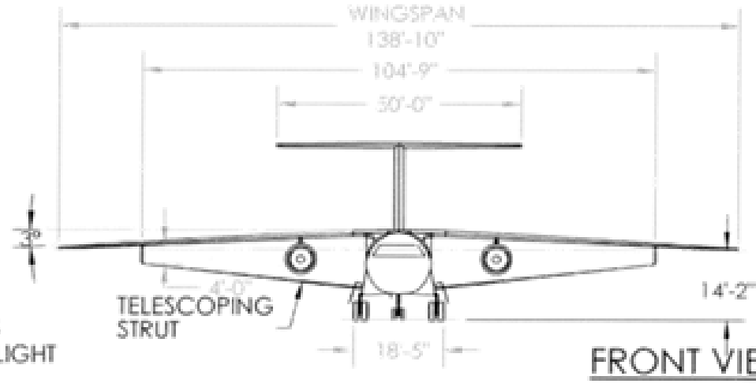

FRONT VIEW

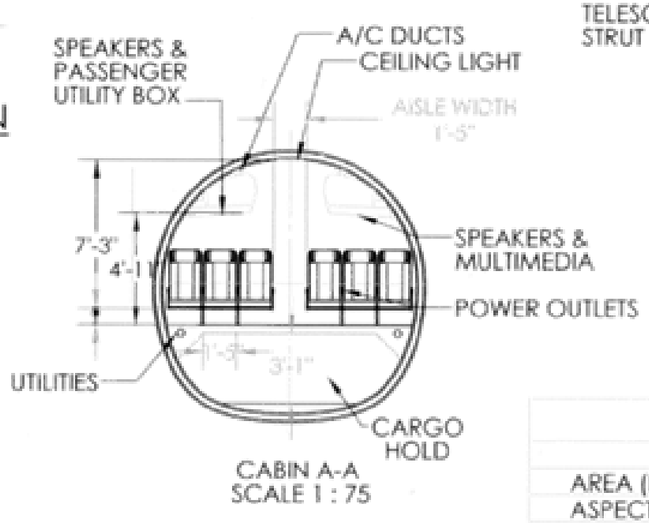

CABIN A-A
SCALE 1 : 75

CABIN CROSS SECTION

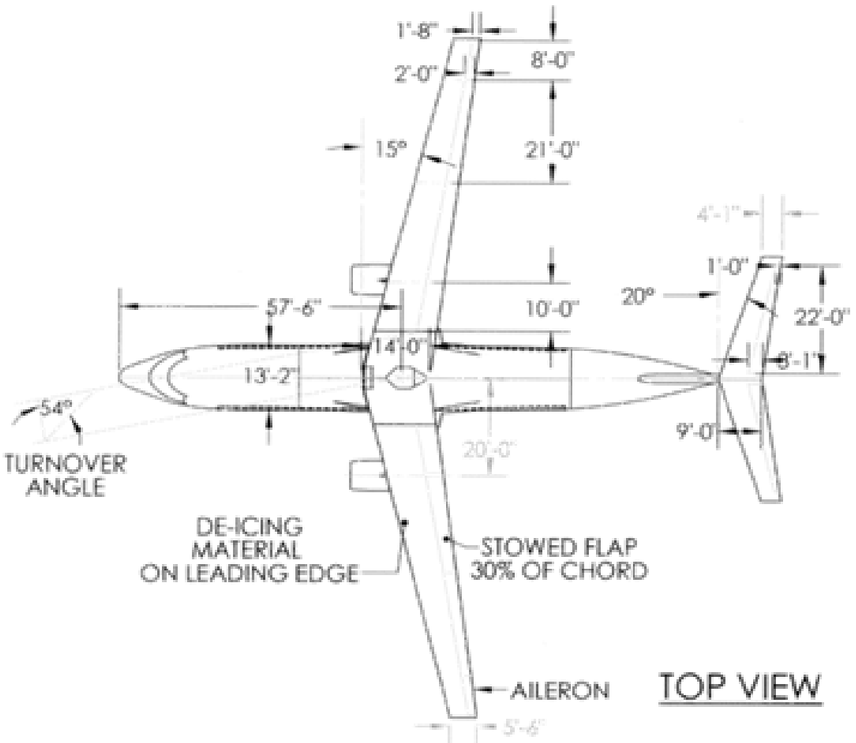

TOP VIEW

SEATING CHART

DATA SUMMARY			
	WING	HORIZ TAIL	VERT TAL
AREA (REFERENCE)	1296 FT^2	334 FT^2	236 FT^2
ASPECT RATIO	15.12	7.5	1.37
TAPER RATIO	0.39	0.45	0.50
SPAN	140 FT	50 FT	18 FT
ROOT CHORD	14 FT	9 FT	18 FT
TIP CHORD	5.5 FT	4 FT	9 FT
MEAN AERO CHORD	9.92 FT	8.08 FT	15.69 FT
DIHEDRAL ANGLE	3°		
SWEEP AT LEAD EDGE	15°	20°	38°
SWEEP AT 1/4C	16°	17°	38°
T/W RATIO	0.252		
TOGW	123,379 LB (1200NMI)/ 131,381 (2200NMI)		
MAIN LANDING GEAR	44.5 X 14.5 TYPE VII X 4		
NOSE LANDING GEAR	27 X 7.75 TYPE VII TIRES X 2		

UNLESS OTHERWISE SPECIFIED:
DIMENSIONS ARE IN INCHES
TOLERANCES:
FRACTIONAL ±
ANGULAR: MACH ± BEND ±
TWO PLACE DECIMAL ±
THREE PLACE DECIMAL ±

	NAME	DATE
DRAWN	TCM	5/5/2010
CHECKED	BSL	5/5/2010
ENG APPR.		
MFG APPR.		
Q.A.		
COMMENTS:		

INTERPRET GEOMETRIC TOLERANCING PER:
MATERIAL
FINISH
DO NOT SCALE DRAWING

PROPRIETARY AND CONFIDENTIAL
THE INFORMATION CONTAINED IN THIS DRAWING IS THE SOLE PROPERTY OF CP AERONAUTICS. ANY REPRODUCTION IN PART OR AS A WHOLE WITHOUT THE WRITTEN PERMISSION OF CP AERONAUTICS IS PROHIBITED.

TITLE:
CP-01

SIZE B | DWG. NO. 3 View | REV
SCALE: 1:350 WEIGHT: | SHEET 4 OF 5

Figure 2.6 CP-01 Planeteer 3-view

3 Aerodynamics

To design an aerodynamically sound aircraft, several criteria must be met. First and foremost, an airfoil must be chosen to achieve a 25% increase in lift-to-drag ratio. This study was conducted using several design analysis codes including TSFoil[52] and XFoil[53]. It is also important to keep in mind that the desired airfoil must exhibit natural laminar flow technology. In addition to the airfoil selection, a proper wing design also plays a significant role in the overall aerodynamic performance of the Planeteer. The overall wing design will be discussed as well as aspects such as wing sweep and wing thickness. Finally, each source of drag affecting the aircraft will be analyzed.

3.1 Airfoil Theory

As stated before, the CP Aeronautics airfoil team utilized several aerodynamic design optimization codes to assist in choosing the correct airfoil. At least eight different airfoils were scrutinized placing an emphasis on lift coefficient and pressure distribution. Below is a figure of the target pressure distribution that a supercritical airfoil undergoing transonic airspeeds should exhibit.

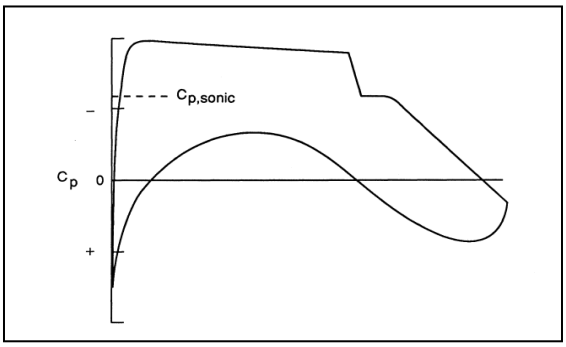

Figure 3.1 Typical supercritical airfoil pressure distribution at transonic speeds[12].

With Figure 3.1 in mind, airfoils were categorized based on similar pressure distributions. TSFoil was used to accomplish this task. This program is a 2-D transonic airfoil analysis code which requires coordinates of an airfoil for a test to be run. The program allows the user to input several different flight conditions including angle of attack, Mach, and Reynolds number. After running several tests for each airfoil the team considered, one pressure distribution graph stood out among the others (as explained below).

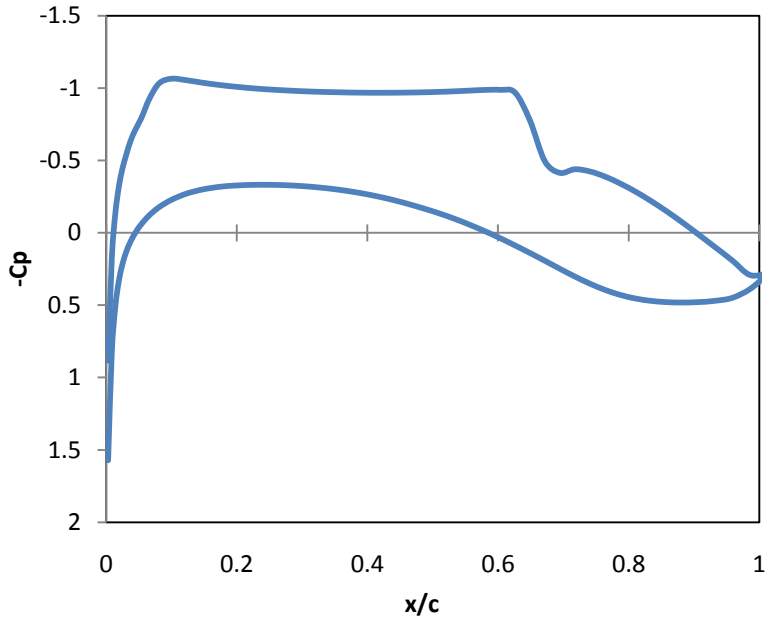

Figure 3.2 Pressure distribution for SC(2)-1010 airfoil at M=0.8, α=0˚.

This pressure distribution as seen in Figure 3.2 is very similar to that of the target distribution in Figure 3.1. This airfoil, the SC(2)-1010, is a NASA supercritical airfoil whose coordinates were obtained from a NASA technical paper[12]. Having passed the first test with a desirable pressure distribution profile, the next step was to analyze the lift coefficient this airfoil could produce.

It is important to note again that this program is a 2-D, or unswept wing, calculator, therefore the swept wing values used as inputs, must be converted to unswept values beforehand. Below is a series of conversion equations.

$$M_{unswept} = M_{swept}\, cos\Lambda \tag{3.1}$$

where $M_{unswept}$ is the unswept wing Mach number, M_{swept} is the swept wing free stream Mach number and Λ is the leading edge sweep angle. Next for the thickness to chord ratio,

$$(t/c)_{unswept} = \frac{(t/c)_{swept}}{cos\,\Lambda} \tag{3.2}$$

where $(t/c)_{unswept}$ is the unswept thickness to chord ratio with corresponding swept thickness to chord ratio, $(t/c)_{swept}$. Lastly, once the program has finished a test run, it outputs unswept lift coefficient. To include wing sweep effects, the following relation is used,

$$C_{L_{swept}} = C_{L_{unswept}}\, cos^2\Lambda \tag{3.3}$$

where intuitively, C_{Lswept} and $C_{Lunswept}$ are the swept and unswept lift coefficients respectively. It is essential to point out that each unswept property is the value the aircraft "sees" perpendicular to the leading edge of the wing.

Using TSFoil again under the same flight conditions, an unswept lift coefficient of 0.72 was predicted, yielding a 0.64 swept wing lift coefficient for this airfoil (note: at zero angle of attack). This was ultimately the highest lift coefficient computed out of the whole set of airfoils being tested. This made the decision of CP Aeronautics quite clear to use this airfoil. The figure below illustrates the profile of the SC(2)-1010 airfoil.

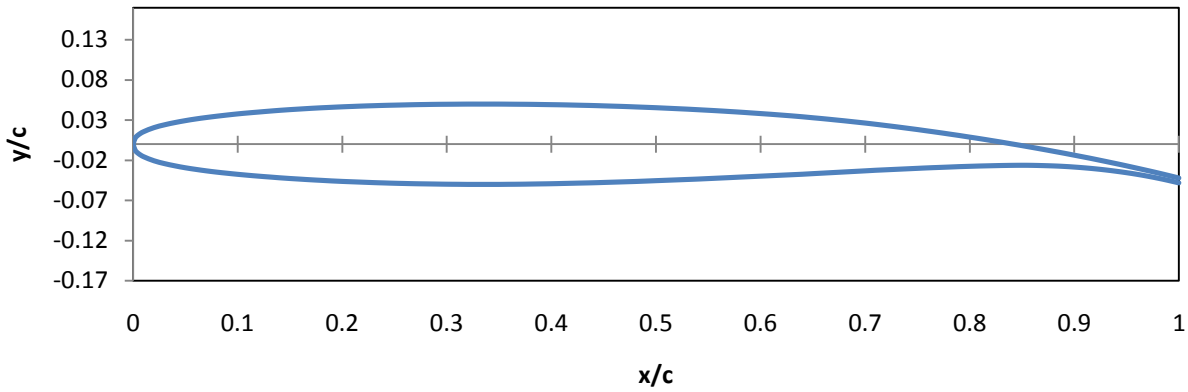

Figure 3.3 SC(2)-1010 airfoil profile.

An important aspect to note is the airfoil thickness. The thickness to chord ratio, t/c, of this airfoil is 10%. This percentage is generally smaller than that of typical commercial passenger jets. It is essential to remember that the presence of the strut reduces the need for structural reinforcement at the wing root as well as decreases thickness to chord ratio, conserving material and money and developing a more aerodynamic profile.

3.2 Laminar Flow Control

One of the major stipulations of the RFP is to achieve an increase in L/D through novel configuration and the use of laminar flow control. Increased laminar flow has long been known to be an effective method for decreasing the profile drag of an aircraft, but has never really been implemented in commercial transport design due to the complexity and cost associated with it.[1] Many of these issues are largely due to structural complexities resulting in increased wing weight which canceled out any gains in fuel burn due to decreased drag. However, the implementation of a strut could prove to be an effective way of mitigating these complexities and achieving the desired increase in performance. Next, it is appropriate to examine why laminar flow is advantageous, and what mechanisms influence it.

The characterization of laminar or turbulent pertains to the nature of the flow within the boundary layer, and it is largely determined by the Reynold's number. There are two important factors that contribute to drag which are influenced by the nature of the boundary layer: skin friction, or surface sheer, and the momentum thickness.

Another important contributor to drag is momentum thickness and its relation to the pressure distribution over the airfoil. A typical transonic airfoil forms a shock wave at or near cruise speeds due to the flow accelerating up to and past Mach 1 over the surface. This in itself causes a significant increase in drag, known as wave drag, but it also greatly increases the momentum thickness which induces turbulent flow and gives rise to more significant amounts of pressure drag. It is therefore a major objective of laminar flow control to shape the pressure distribution in a way such as to minimize the growth in momentum thickness, and thus maintain laminar flow.

There are two methods of flow control: natural laminar flow control (NLFC) and hybrid laminar flow control (HLFC). NLFC employs the use of the airfoil geometry to maintain laminar flow as long as possible. HLFC uses geometry as well as a system of mechanisms to remove mass from the flow, called suction, thus changing the boundary layer parameters and prolonging laminar flow. Figure 3.4 and **Error! Reference source not found.** demonstrate the pressure distribution and momentum thickness characteristics of an HLFC transonic airfoil versus a traditional fully turbulent one.

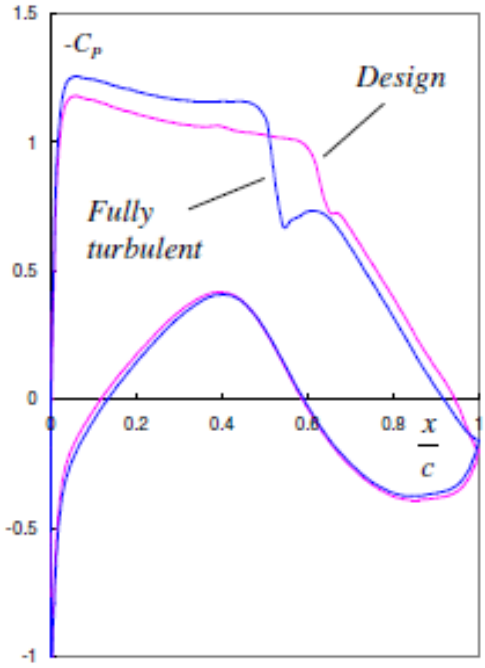

Figure 3.4 Pressure distributions of HLFC and fully turbulent airfoils at the Same M and C_L.[13] "Design" distribution used as reference for Planeteer's airfoil selection.

Looking at Figure 3.4, it is seen that the pressure coefficient on the suction side towards the front is reduced slightly. The shock is pushed back and mitigated due to the lower Mach number ahead of it, and thus the pressure drag is lowered. This pressure distribution, labeled "design", provided a reference for analyzing and selecting the Planeteer's airfoil.

CP Aeronautics decided to incorporate NLFC instead of HLFC based on the fact that HLFC significantly enhances the complexity of the interior wing structure and adds additional weight in pumps and tubing to remove mass from the flow. In addition, transonic airfoils being thin by nature are already hard pressed for free space, and the implementation of fuel tanks into the wings provided little or no vacancy for a complex system of pumps and hoses. Furthermore, the Planeteer is optimized to NLFC due to its already relatively high aspect ratio and lower sweep. These were two of the major parameters that challenged earlier studies. One of the leading contributors to the introduction of turbulence is cross flow, which is greatly mitigated by a lower sweep. A higher aspect ratio and its implication of a shorter chord is also conducive to keeping the flow laminar for a larger percentage of the chord and lowering the Reynolds number.

Using NLFC however poses its own challenges; specifically manufacturing and maintaining smooth, clean leading and suction surfaces. One guiding assumption of the design is that industry manufacturing techniques and materials will be up to par with the requirements of natural laminar flow. Another problem to take into consideration is the contamination of the surfaces by dead insects. This is a very real threat to natural laminar flow and a satisfactory solution may be very complicated. Such a solution is not outlined in this report but would certainly be an important area of investigation and experimentation for the next step of the design.

3.3 Max Lift Coefficient

Figure 3. gives the lift curve for the NASA SC(2)-1010 transonic airfoil at a Reynolds number of $1.5x10^7$ and a Mach number of 0.21. These are the conditions representative of landing and take-off, the context in which this analysis was relevant. The points were produced using the viscid flow analysis in XFoil. More points were computed and plotted around the peak of the curve. With this, the two dimensional $C_{l\,max}$ was determined to be 2.18 occurring at an α of 14 degrees. Factoring in wing sweep the, max lift coefficient is 2.04. The lift curve slope ($dC_L/d\alpha$) was also determined from this analysis to be 0.1188.

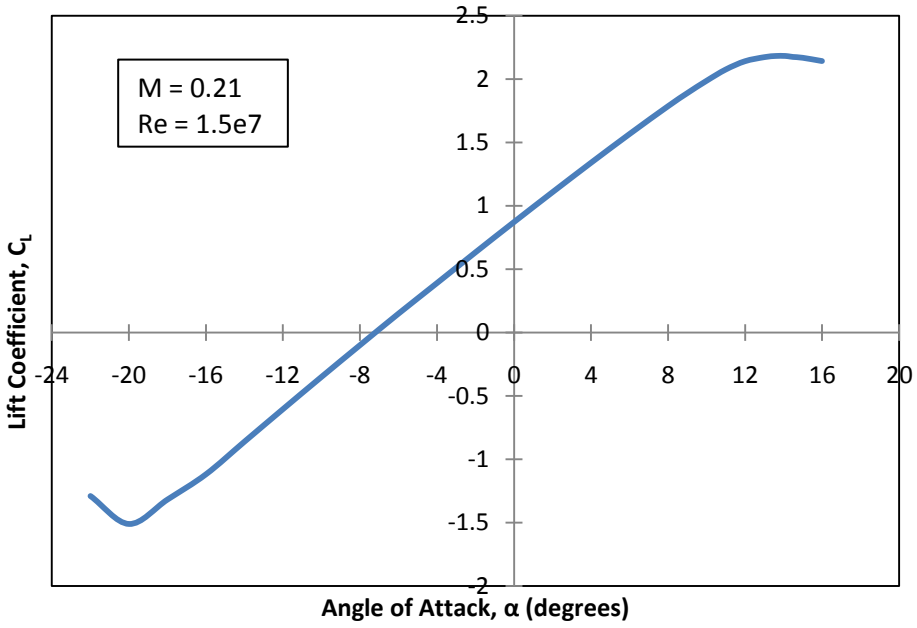

Figure 3.5 Lift Curve for NASA SC(2)-1010 transonic airfoil at subsonic speed (XFoil).

3.4 Wing Design

With such a high goal for lift-to-drag ratio, the wingspan of the Planeteer will undoubtedly need to be elongated in comparison to its Boeing 737 counterpart. The wing span of the 737 is approximately 117 feet, whereas

the wing span of the Planeteer was chosen to be 140 feet. The implementation of the strut must be credited to achieve this wingspan. As stated in section 2.3, the strut allows for the overall weight of the aircraft to be decreased since less material is needed to reinforce the wing root as well as the section of the wing inboard of the strut attachment. In addition the airfoil thickness can be decreased due to increased structural support of the wing. With so much weight savings, there is much room to increase the wingspan. It is also important to note that the critical Mach number location is delayed along the chord length with decreased airfoil thickness. This is a desirable feature since the amount of laminar flow over the wing is increased and in effect, decreasing the wave drag. Likewise, decreased wing sweep also helps to delay the location of critical Mach number. Therefore, the leading edge wing sweep of this wing was chosen to be 15˚, a full 15˚ smaller than that of the 737. In essence, this counts as another weight saver.

Another significant aspect of the wing design is its overall geometric shape. Most often, commercial airliners will have a large root chord with a trailing edge, near the fuselage, running perpendicular to the fuselage. This perpendicular trailing edge will span the area of the wing containing the landing gear, after this point, the trailing edge usually continues according to the predefined taper ratio. However, with the strut in place, the wing is mounted as a high wing and will not house any landing gear machinery, therefore, it is unnecessary to have trailing edge section perpendicular to the fuselage. Instead, the trailing edge will sweep back at a constant angle following a taper ratio of 0.39 with a root chord of 14 feet. The final design yields a planform of 1296 square feet and an aspect ratio of 15.12. This high aspect ratio will ultimately lead to a higher lift-to-drag ratio.

3.5 High Lift Devices

To allow a wing better optimized for cruise, the Planeteer is equipped with a high-lift system to allow take-off and landings at lower speeds than the wing would otherwise allow. Simpler systems greatly reduce manufacturing and maintenance costs, and so the Planeteer uses relatively simple Fowler flaps, affecting roughly 77% of the wing, with the flaps increasing the chord of the wing by about 40% when extended. The flap hinge line is swept at approximately 20°. The Planeteer is not equipped with any leading edge devices.

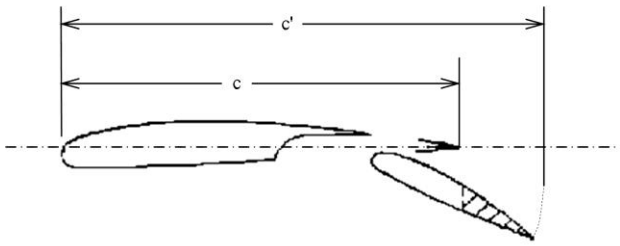

Figure 3.6 Generic wing section with a Fowler flap[51]

Raymer suggests Equation 8.1 to estimate the change in $C_{L,max}$ provided by the flaps.

$$\Delta C_{L_{max}} = 0.9\Delta C_{l_{max}} \left(\frac{S_{flapped}}{S_{ref}}\right) \cos \Lambda_{\text{H.L.}} \tag{3.4}$$

Raymer also indicates that for Fowler flaps, $C_{l_{max}} = 1.3 * c'/c$[8]. This high lift system provides a $\Delta C_{L_{max}}$ for the Planeteer of approximately 1.19, resulting in a total $C_{L_{max}}$ for the aircraft of 3.29.

The relatively simple Fowler flap, and the lack of leading edge devices, will appreciably decrease manufacturing costs and maintenance costs by offering a much simpler wing, when compared with existing aircraft of this class, which typically have compound trailing edge devices in addition to leading edge slats or flaps.

3.6 Aircraft Drag

To account for the entire drag of the aircraft it is necessary to look into the major types of drag that are dominant at transonic cruise speeds. These include parasite drag, induced drag and wave drag. The complete drag equation is derived below,

$$C_D = C_{D,0} + KC_L^2 + 20(M_\infty - M_{crit})^4 \tag{3.5}$$

where $C_{D,0}$ is parasite drag, KC_L^2 is induced drag, and $20(M_\infty - M_{crit})^4$ constitutes as the wave drag, which will later be represented as C_{Dw}[13]. To clarify a few terms, K is equivalent to $1/(\pi AR e)$ (where AR is aspect ratio and e is the Oswald efficiency factor), C_L is the lift coefficient, and M_{crit} is the critical Mach number. Usually wave drag would not be factored into this equation, however since the aircraft will be traveling transonic, this is a necessary addition.

To evaluate parasite drag, another analysis code titled Friction is used[54]. The program requires several inputs including the wetted area of each main surface of the aircraft and corresponding reference lengths, reference surface area and the Mach and altitude the aircraft is flying. Using a Mach of 0.8 and an altitude of 40,000 ft, a parasite drag of 0.0145 is calculated.

To begin the analysis of the wave drag, the critical Mach number must be solved for which is given by the equation below,

$$M_{crit} = M_{DD} - \left(\frac{0.1}{80}\right)^{1/3} = M_{DD} - 0.1077 \tag{3.6}$$

where M_{DD} is the drag divergence Mach number[13]. Once again, there is an unknown term, M_{DD}, which may be solved for using the modified Korn equation which has been manipulated to include sweep angle,

$$M_{DD} = \frac{\kappa_A}{\cos \Lambda} - \frac{(t/c)}{cos^2 \Lambda} - \frac{C_L}{10 cos^3 \Lambda} \tag{3.7}$$

where κ_A is an airfoil technology factor which has a value of 0.95 for a supercritical section and *(t/c)* is the thickness to chord ratio[13]. As stated before, the leading edge wing sweep of this aircraft is 15˚, the thickness to chord ratio is 0.10 once again and the unswept wing lift coefficient will be that of the airfoil obtained from TSFoil, 0.64. Entering in each parameter yields a value of 0.82 for M_{DD}. Next, M_{crit} is found to be 0.71. Figure 3. shows the drag divergence, or drag rise, break down.

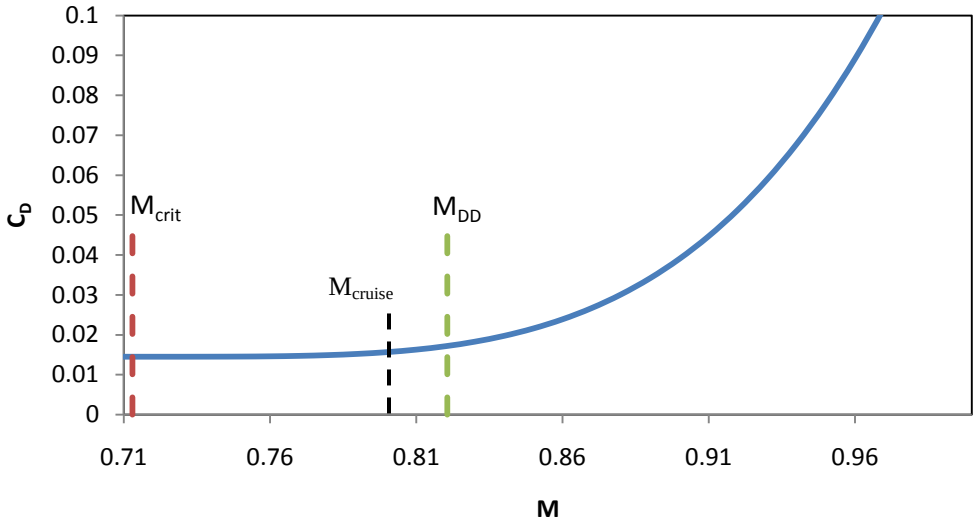

Figure 3.7 Drag divergence.

At this point, the wave drag can now be calculated as a function of lift coefficient. The comparison of the parasite, induced and wave drag can be seen in the drag polar below.

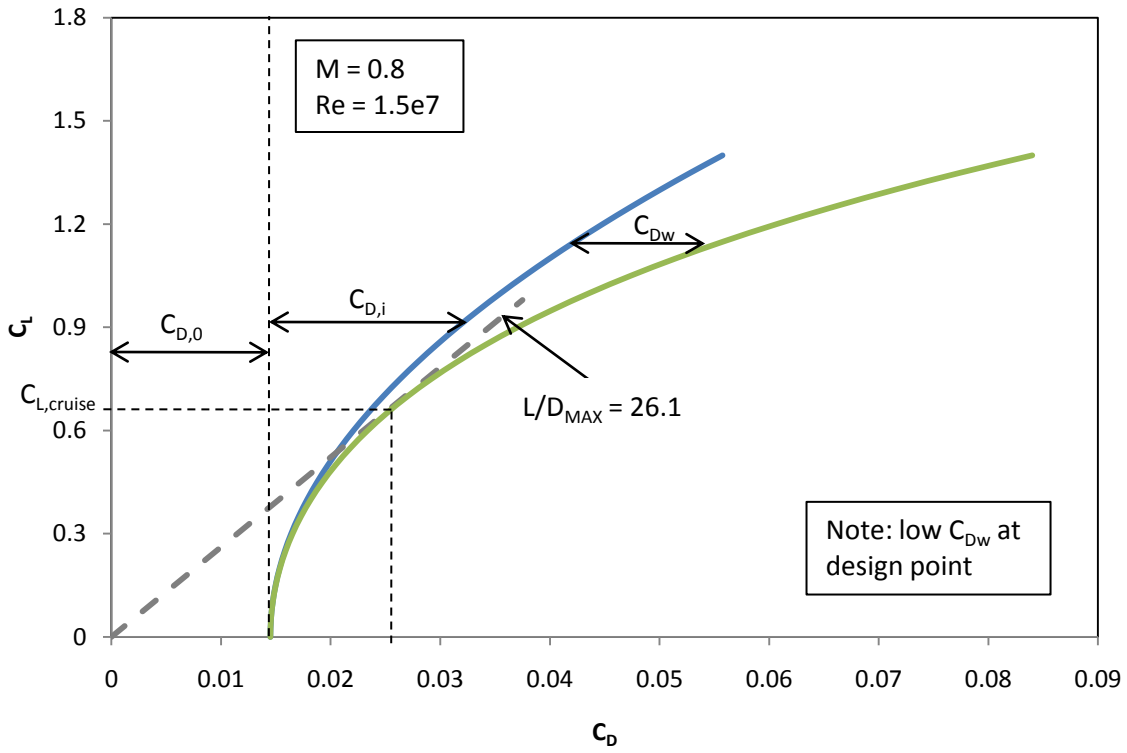

Figure 3.8 Drag Polar during cruise.

The blue curve is the drag profile neglecting wave drag and the green curve includes wave drag. For the purposes of this aircraft design, the L/D_{MAX} (the maximum lift-to-drag ratio the Planeteer may achieve incurring wave drag) obtained from the green curve is used to obtain the design lift-to-drag ratio, which is 26.1. This value is significantly higher than that of a Boeing 737 or Airbus A320 and more importantly much greater than a 25% improvement.

4 Propulsion

The RFP requires a cruise Mach number of 0.8. The primary engine selection criteria include efficiency, reduction in engine noise, and reduction of emissions. The two engines in consideration are the PW1000G geared turbofan and the GE-36 open rotor design. The engine data for each model is shown in Table 4.1.

Table 4.1 Performance Characteristics of Proposed Engines[16,17].

Engine	PW1000G	GE-36
Type	Geared Turbofan	Open Rotor
Thrust (lbs)	17000-23000	25-30% less than current
Cruise SFC	22-23% better than current	25-30% better than current
Bypass Ratio	12	50
Weight (lbs)	4500	5010
Fan Diameter (in.)	73	120
Engine Length (in.)	Less than current	Same as current

4.1 PW1000G Geared Turbofan

The PW1000G uses a gear box to separate the engine fan from the low pressure compressor and turbine, allowing each of the modules to operate at their optimum speeds. This allows the fan to rotate slower while the low pressure compressor and turbine operate a high speed, increasing engine efficiency and delivering significantly lower fuel consumption, emissions and noise. This improved efficiency also translates to fewer engine states and parts for lower weight and reduced maintenance costs[16]. Pratt & Whitney expects the PW1000G to provide a 22-23% fuel efficiency gain by 2017[17].

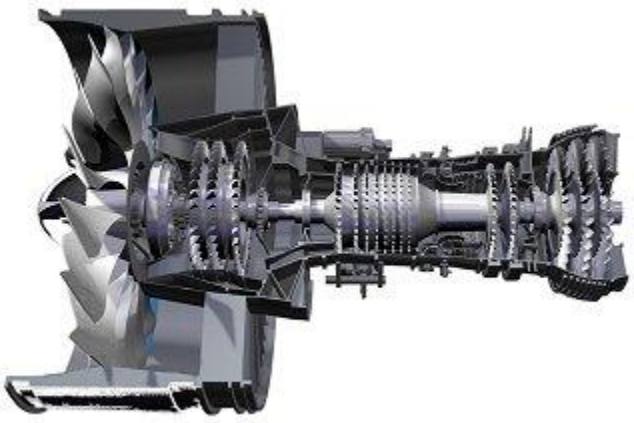

Figure 4.1 PW1000G[18]

4.2 GE-36 Open Rotor

The GE-36 is a modified turbofan engine in which a gas-turbine core drives a large-diameter fan which propels large amounts of cool air around the outer part of the engine. This creates a very high bypass ratio and thereby considerably increases the efficiency of the engine over conventional turbofans. GE claims that their open rotor design will perform 25-30% better than current turbofans. An aircraft powered by an open rotor is likely to have a cruising speed 5-10% than a turbofan powered aircraft. While this will reduce operating noise, vibrations from the exposed fan blades produce a considerable amount of noise, nullifying the reduction from slower cruising speeds and making the engine significantly louder than comparable turbofans.[18]

Figure 4.2 GE-36[19]

4.3 Engine Selection

The efficiency of current technology turbofans is improving at an average of 1% a year. This means that the turbofan engines available in 2020 are likely to be at least 11% more efficient than today's models. The PW1000G will provide at least an 11% increase in fuel efficiency over conventional engines while the GE-36 will produce at least a 14% increase. The PW1000G will be able to meet the RFP cruise speed requirement of Mach 0.8. The GE-36 will require the Planeteer to operate at a speed slower than the speed which the RFP requires. The PW1000G will have reduced engine noise compared to conventional turbofans while the GE-36 will have increased noise.

The PW1000G geared turbofan was selected based on the engine selection criteria and the RFP requirements. While the GE-36 has a better efficiency, the PW1000G provides the best reduction in noise and engine weight while having comparable thrust values and operating Mach number to conventional turbofans.

4.4 Engine Installation and Access

Each engine is installed in a nacelle 20 feet from the centerline of the fuselage. The nacelles hang under the wing from traditional pylons. Since the engines are further from the ground than those on a conventional low-wing airliner, step-ladders will be necessary for regular engine maintenance.

5 Initial Weights

5.1 Initial Weight Estimation

With a design point chosen by the thrust-to-weight and wing loading diagram, and PW-1000G engines, an initial estimate for the TOGW of the Planeteer can be made. By using the method described in Chapter 6 of Raymer's text, a Matlab program was written to computed an initial TOGW, empty weight and fuel weight for the Planeteer (while following the mission profile)[20]. Below is a table of assumptions and reasons for the assumption that was used in the program:

Table 5.1 Assumptions for initial weight calculations

Assumption	Reason
W/S = 110	Design point chosen
T/W = 0.25	Design point chosen
22% reduction in SFCs	Advanced engines (PW1000G)
Multiply Empty Weight Fraction by 90%	Composite Structures
Cd_0 = 0.0198	Initial drag estimation
Cruise altitude at 40k ft	Best cruise altitude
Crew weight is 1,400 lbs	7 crew members (2 pilots, 5 attendants) 200 lbs each (person and luggage)
Full payload of 37,000 lbs	Required by RFP
Fuel weight is calculated is to complete the mission profile with 6% fuel in reserve	Raymer recommendation for 6% fuel in reserve

By using these assumptions, the initial weights were found to be:

Table 5.2 Initial ("design") weight results

Weight	(lbs)
TOGW	142,462
Empty weight	70,484
Fuel weight	33,578

These weights will be used as the "design" weights for aircraft loads in the structures section.

6 Materials

6.1 Control Surfaces

Control surfaces will be constructed of 2024-T0 aluminum alloy. The reason for using this instead of CFRP (Carbon Fiber Reinforced Plastic) is primarily a cost saving measure. Control surfaces are not under relatively high loads and the reasonable strength offered by aluminum will get the job done at a cheaper price than CFRP with only a slight weight penalty. In addition, the high thermal conductivity of aluminum is useful for when deicing becomes necessary. Finally, having the wing's leading edge slat made of aluminum will allow for easy repair in the event of bird strikes. Repair to aluminum is a much simpler process than repairing CFRP and if replacement of the slat is required, this can be more cheaply accomplished using aluminum.

6.2 Aircraft Skin

The skin of the aircraft, wrapped around an aluminum alloy frame, will be primarily constructed from CFRP due to the impressive weight savings it offers. Although slightly pricier, CFRP is the right material to use when weight is of upmost importance. In the fuselage skin alone, a weight savings of 810 lbs can be expected by using CFRP instead of 2024-T0 aluminum alloy. This makes the total fuselage skin weight 43% lighter when made out of CFRP than one constructed of aluminum. Non-loaded fairings will be constructed from fiberglass to keep weight and cost at a minimum. These include the landing gear pods, the fairing covering the mating of the wing to the fuselage, and the radar dome. Constructing the radar dome from fiberglass will allow cheap, easy repairs in the event of a bird strike as well as easy penetration of the aircraft's radar system.

6.3 Landing Gear

The landing gear, when extended, will protrude from the non-loaded fiberglass pods and attached to the applicable bulkhead using a high strength Ti Alloy, AMS 4914. The landing gear will be constructed from AF140 Steel for its nearly unbeatable yield strength. This particular type of steel also exhibits above average corrosion resistance when compared to similar ferrous alloys. This resistance will be necessary when operating on a rain soaked runways when the gear get wet.

6.4 Manufacturability

The manufacturability of this aircraft will be straight forward when taking into account modern and future composite manufacturing techniques. CFRP can be made into virtually any shape and is extremely corrosion resistant and strong. Although more expensive than aluminum alloys, the ease of construction of composite parts will help ease the price burden of the raw material. CFRP can be manufactured with very little waste material. Aluminum on the other hand, has to be drilled and cut and therefore large amounts of material are thrown away. Another alternative, titanium, presents its own host of issues. Although rivaling CFRP in strength, the treatment process of titanium is expensive and complex. Titanium is annealed at well over 1000°F and is vulnerable to material imperfections that may weaken the material or make it susceptible to brittle fracture. When considering the manufacturability of the fuselage's frame, we decided to use aluminum for cost savings. The 9.175 psi max cabin pressurization at FL410 did not warrant the higher strength CFRP to be used and the CRFP skin can easily be fastened around an aluminum frame, easing delays on the assembly line.

A comparison of the different materials being used in the Planeteer can be seen in Table 6.1 below.

Table 6.1 Material Properties Comparison[27]

Property	Al Alloy 2024-TO	Al Alloy 7075-TO	CFRP	AF1410 Steel	Ti Alloy AMS 4914	Ti-6A-4V Annealed
Yield Strength (KSI)	10.9	15.2	79.8	226.3	110.4	15.2
Compressive Strength (KSI)	10.9	15.2	82.5	237.9	110.7	15.2
Density (lb/ft^3)	172.8	174.7	98.6	488.6	297.0	174.7
Thermal Conductivity (lb/s-°F)	24.1	16.8	0.2	3.6	1.0	16.8
Water	Very Good	Very Good	Very Good	Good	Very Good	Very Good
Cost ($/lb)	1.29	1.25	25.82	5.41	38.43	1.25
Relative Cost (x-times more expensive)	1.0	1.0	20.7	4.3	30.9	1.0
Cost ($/ft^3$)	222.10	217.28	2,542.32	2,639.58	11,401.08	217.28
Volumetric Relative Cost	1.0	1.0	11.7	12.1	52.5	1.0

A distribution of materials used can be seen in Figure 6.1 below.

Fiberglass	BLUE
CFRP	GREEN
Aluminum	GREY

Figure 6.1 Materials Used

7 Structures

The goal of Planeteer's structures is to reduce weight while following all required safety guidelines for structural integrity throughout the entire mission. The goal will be realized by using advanced materials and a strut braced wing to reduce the overall weight.

7.1 Previous Research of Strut Braced Wings and Constraints

Research conducted at Virginia Tech by Maarten van Hoek and Amir Naghshineh-Pour will provide design guidelines and principles on integration and structural layout of Planeteer's strut-braced wing. The only constraints to be made at this point will be that the engines will be mounted under the wing and located 20ft from centerline of the aircraft.

7.2 Vertical Offset Consideration

Typical strut-wing configurations from Naghshineh-Pour's research are provided in the figure below:

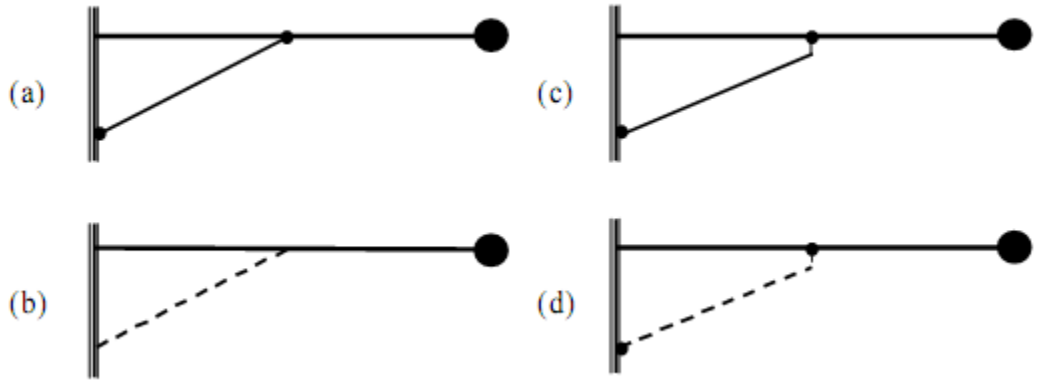

Figure 7.1 Strut-braced configurations[21]

As seen from Figure 7.1(a) and (b) have no vertical offset while (c) and (d) have a vertical offset. Naghshineh-Pour writes that research shows that the configuration show in Figure 7.1 (a) would produce large interference drag at the sharp angle where the strut meets the wing[21]. Therefore, to reduce this drag the sharp angle is eliminated in Figure 7.1(d) and a vertical offset is used to decrease this drag. Below is a figure describing the vertical offset:

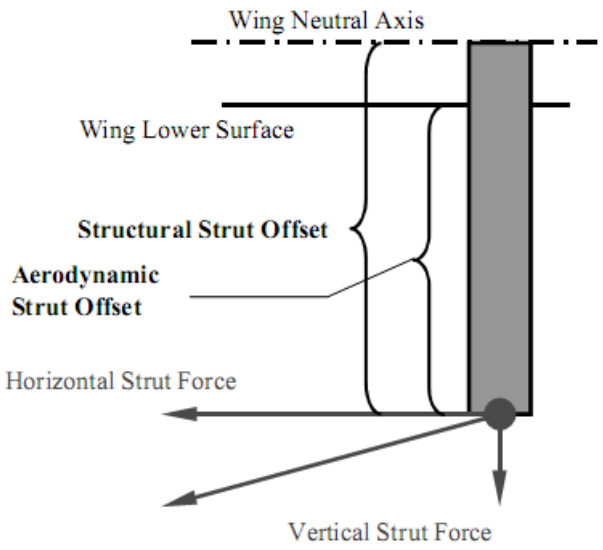

Figure 7.2 Description of the vertical offset

The structural length of the vertical offset will be decided by the results of Naghshineh-Pour's research. The figure below describes the optimum offset length for the least interference drag and weight:

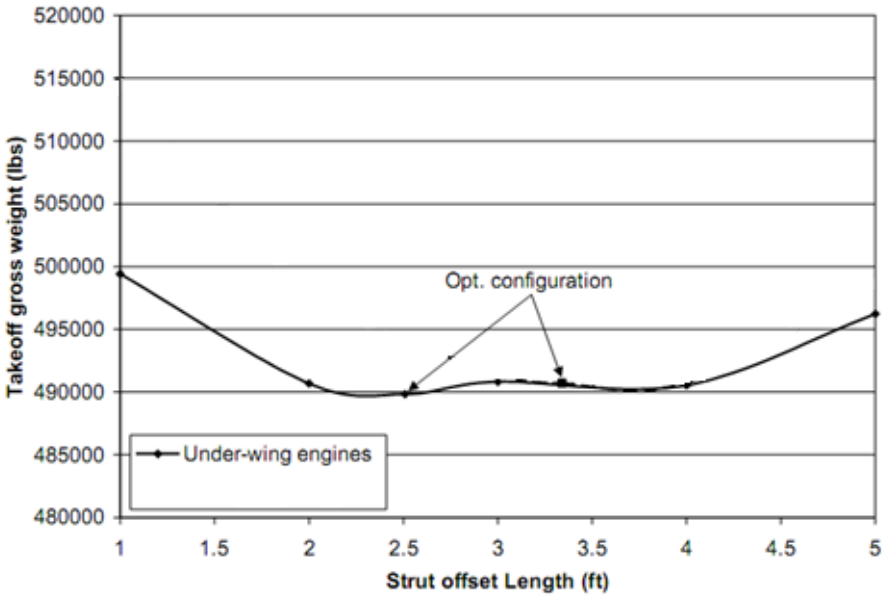

Figure 7.3 Results from Naghshineh-Pour's research for offset length[21]

From these results (under-wing engines) and a geometric constraint from the placement of the engines and their pylon length, the vertical offset length was chosen to be 4 feet. This will be aerodynamic offset length that will be used in the Planeteer's design.

7.3 Strut Cross Section

The cross section of the strut will be a symmetric airfoil so that the strut would cause a minimal amount of lift as the aircraft is flying. To reduce drag, the strut cross sectional area will have a slightly sharp leading and trailing edge with a flat top and bottom surface. This symmetric airfoil will resemble the same cross-section that was found in van Hoek's research[22].

Figure 7.4 Strut member(s) cross-section[22]

7.4 Telescopic vs. Jury Member

The most common issue with using a strut braced wing is the compressive forces sent to the strut during a -1.0g maneuver or a 2.0g taxi bump. These compressive forces would cause the strut to buckle[22]. Two possible solutions have been investigated, incorporating a jury strut member (as shown in Figure 7.5) or use a telescoping member (as show in Figure 7.6) that would cause the strut to "slide in" to itself whenever compressive forces were present[22].

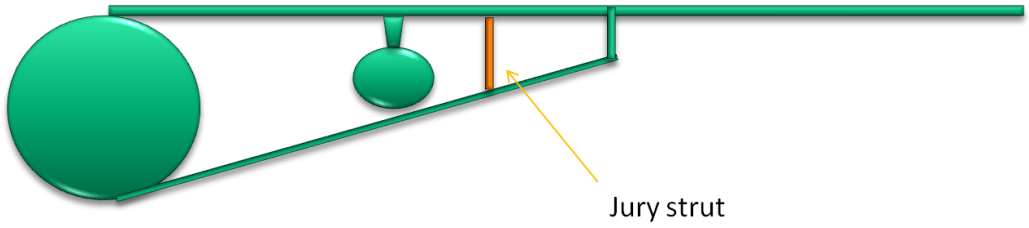

Figure 7.5 Strut stiff member design with jury strut

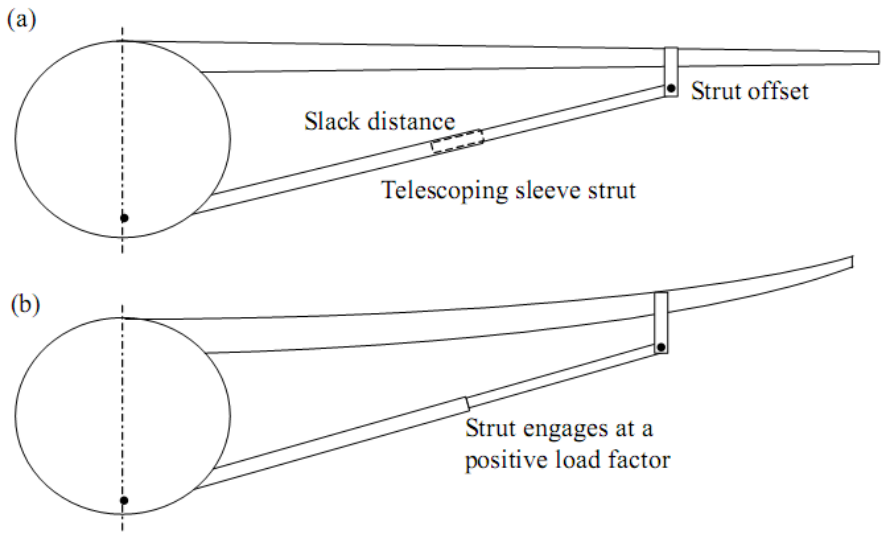

Figure 7.6 Strut with telescoping member design.

Van Hoek's research of the stiff member strut concluded that the optimum three-member stiff design would be mostly inboard of the aircraft as shown in Figure 7.7

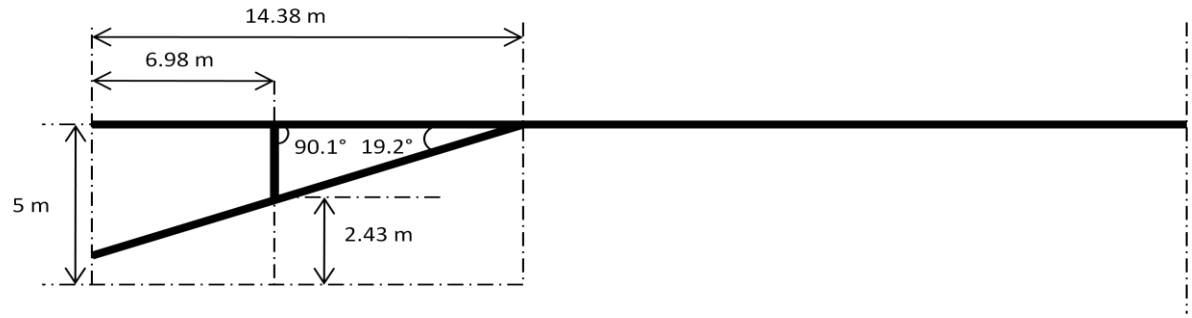

Figure 7.7 Van Hoek's results for a jury member design

Conversely, for a telescoping design in Naghshineh-Pour's research showed that the optimum intersection of the wing and strut is at approximately 70% of the wing half-span as shown in Figure 7.8:

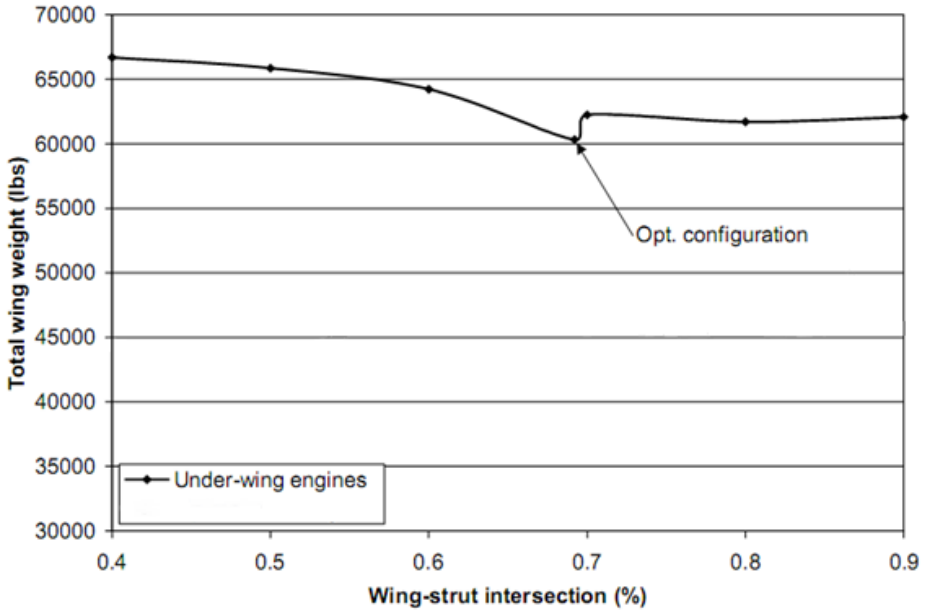

Figure 7.8 Location of wing-strut intersection, for telescope design[21]

Coalescing van Hoek's and Naghshineh-Pour's research, a pro-con chart for a telescope and jury design was made as shown in Table 7.1 and Table 7.2[22].

Table 7.1 Pro-con chart for a jury strut design

Jury Design	
PRO	CON
Simple design	Requires jury strut
Less material possibly needed	Might interfere with engine placement
	Might not be able to withstand a 2.0g taxi bump
	Extra drag from jury strut

Table 7.2 Pro-con chart of a telescope-strut design

Telescope Design	
PRO	CON
Only 2 main members are needed	Might require complex machinery for telescope
Can withstand any negative load, including taxi bump	Possible weight penalty for complexity
Research shows that there are more locations available to place engine	
Takes advantage of a large wing aspect ratio due to wing-strut intersection location at 70% half span	

From these pro-con charts, the research presented, and the constraint that our engine is placed 20 ft from the centerline of the wing, the telescope strut design was chosen for the Planeteer.

7.5 Estimating Wing Weight

The accepted method used to estimate the weight of the wing is by using a two-plate bending model as shown in Figure 7.9:

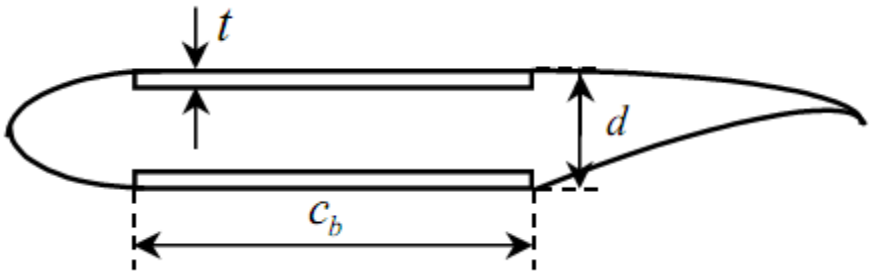

Figure 7.9 Double-plate idealized wing box[21]

This model is used in van Hoek's research because it is assumed "that the wing weight is mainly influenced by the amount of material required to withstand its internal stress due to bending and compression"[22].

7.6 Negative Loads and Telescope Length

Since a telescope design has been chosen, the negative loads are considered negligible in regards to loading on the strut itself. However, since these loads will not be carried by the strut, the wing must act as a cantilever beam to withstand these loads[21,22].

It will be assumed that the -1g maneuver load will be stronger than a 2.0g taxi bump since during the taxi bump, the wing only needs to support itself. During the 1g maneuver, the wing must support the entire weight of the aircraft (including the wing itself). Therefore, when designing the strut, the -1g maneuver will be the more critical case in designing how long the sliding telescoping structure must be.

7.7 V-n Diagram

In order to determine whether the current aircraft can withstand a 2.5g and -1g load with gusts according to FAR 25. A V-n diagram was created using the procedures described in Johnson's and Roskam's text[20,23]. The aerodynamic characteristics of the aircraft, design weight from Table 5.2, gust loads of 66 fps, 50 fps, and 25 fps were used in creating the V-n diagram in Figure 7.10:

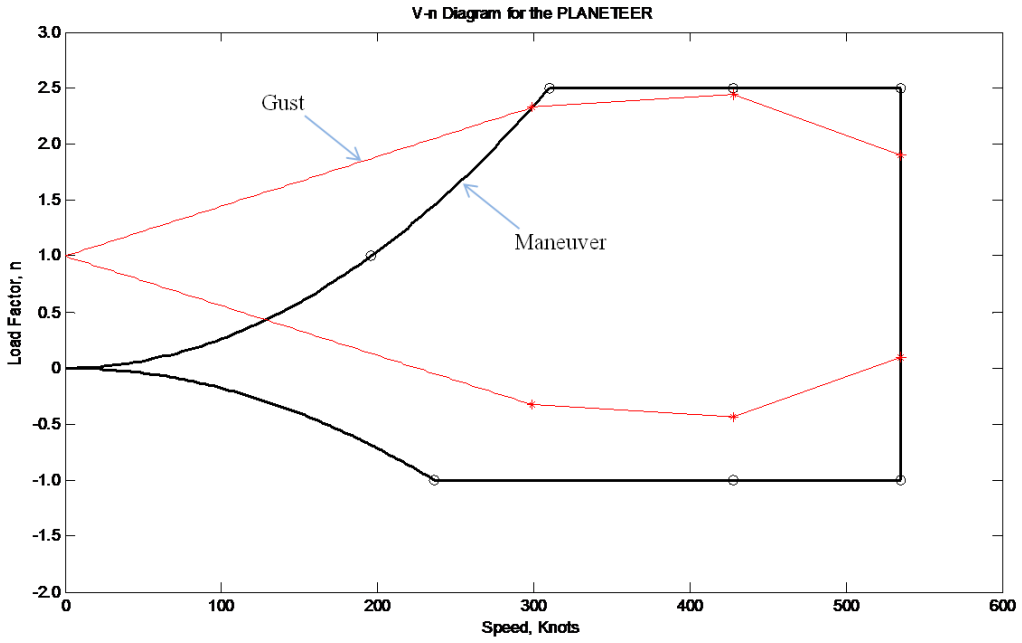

Figure 7.10 V-n diagram.

As the figure shows, the 2.5g and -1g loads that are needed to be accounted for in FAR 25 will also be sufficient when the aircraft experiences a gust.

7.8 Van Hoek Wing-Strut Design Program

Van Hoek has provided a Matlab program that will determine with a given wing geometry, material selection, strut cross sectional area and location: the wing weight, strut weight, and whether the strut will fracture or buckle under those conditions. The program also plots the wing deformation, which will be extremely helpful in determining the length required of the inside telescoping structure.

The program has been modified to fit the Planeteer's dimensions and design criteria. A condensed list of additional modifications and assumptions are presented below in Table 7.3:

Table 7.3 Assumptions and modifications of van Hoek's program

Van Hoek Program Modifications and Assumptions	
The material chosen for the strut and double-plate method is CFRP	Van Hoek's weight penalty of 2.5 for the telescoping member and 1.5 for the non-telescoping member will remain unchanged
A factor of safety of 1.5 will be applied	The minimal plate thickness will be 0.05 in
The current Wing geometry has been implemented	60% of the chord will be assumed to be a plate
The strut will have a vertical offset of 4 ft	An engine located 20 from the root of the wing with an estimated weight of 4500 lbs will be included
The vertical offset/wing intersection point will be located at 70% of the half span	The strut will connect to the fuselage at a point 11 ft from the top of the wing
The program has a telescope design option that will be used	The strut will follow the sweep of the wing
The program has been modified to ignore any effect of the 3rd member so it would not change the results	The cross sectional area of the vertical offset will match the cross sectional area of strut for simplification
Van Hoek uses a weight penalty of 1.1 for the wing. Instead, a weight penalty of 1.2 will be used because of the strut connection to the wing	The total weight of the wing and strut outputted by the program will be multiplied by 2 since the program calculates the weight for only half the wing

7.9 Wing Design Without Strut

Van Hoek's program provides an option to calculate the wing weight without a strut by setting the cross sectional area of the members to zero. This will be used as a comparison to the total wing weight and strut weight to see if the there is reduction in weight between the non-strut wing and the strut-braced wing.

7.10 Wing Design with a Strut

Using van Hoek's program, the required cross sectional for the members was found to be 0.006 m^2. With this cross sectional area, the program indicates that the members will not fracture due to the 2.5g load. The weights of the wing and strut and percent reduction were found to be:

Table 7.4 Estimated weight of the strut-braced wing design.

	With Strut	Without Strut
Strut weight	1,702 lbs	N/A
Wing weight	4,901 lbs	9,994 lbs
Total weight	6,603 lbs	9,994 lbs
Percentage compared to non-strut design	-34%	N/A

As the results show, the strut-braced wing design has a 34% percent reduction in weight compared to the non-braced cantilever wing design. Since the strut needs to telescope inside a "sleeve" the main member will have an outer cross sectional area of 0.007 m^2 and the inside will be 0.006 m^2. The weights will not be needed to be changed since the weight penalties described in Table 7.3 are already considered.

7.11 Wing Deformation

The program plots an estimated wing deformation which will be needed to determine how much "slack" will be needed inside the telescoping member when the aircraft experiences a -1g load. The plotted wing deformation is provided in Figure 7.11:

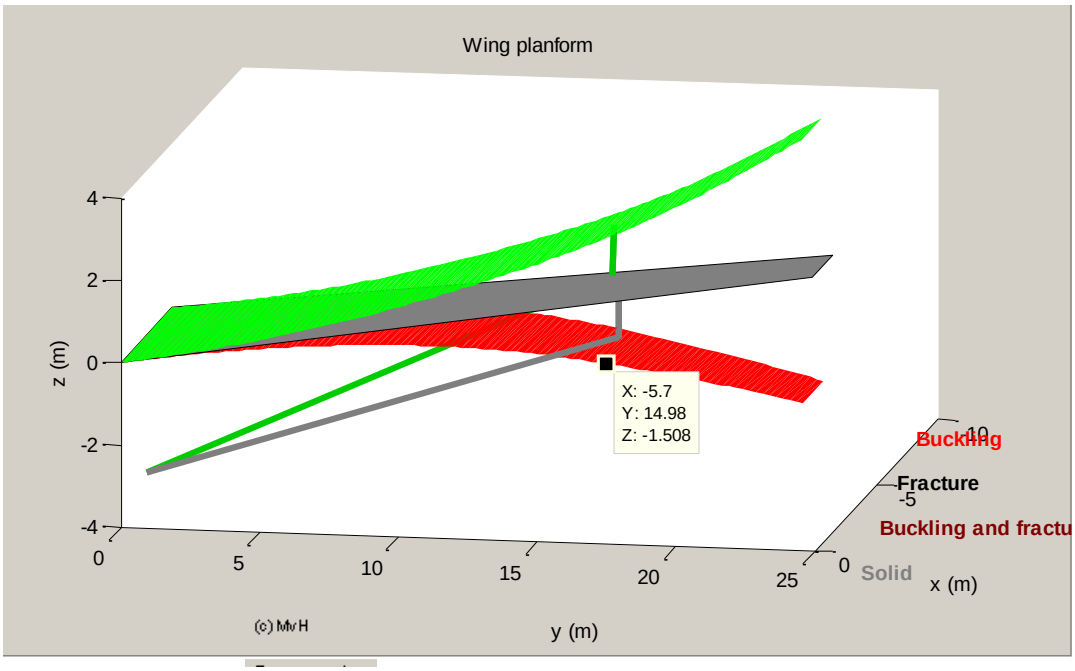

Figure 7.11 The plotted wing deformation provided by the program

As the figure shows, at the approximated location where the strut-wing intersection is located, the deformation due to a -1g load is about 1.5m. For safety, the maximum negative deformation at the point will be increased to 1.6m.

7.12 Final Strut Design and Geometry

Naghshineh-Pour's research suggests that a positive "slack load" be used for any sudden increased positive load experienced by the wing[21]. The main reason for this positive slack is so that the strut is not constantly engaged. Therefore, when the wing is deformed positively such that it pulls the member 3 inches the strut will be engaged in tension.

Combining all the results, the negative wing deformation, and the positive "slack," the final design of the strut-braced wing for the Planeteer is described in Figure 7.12:

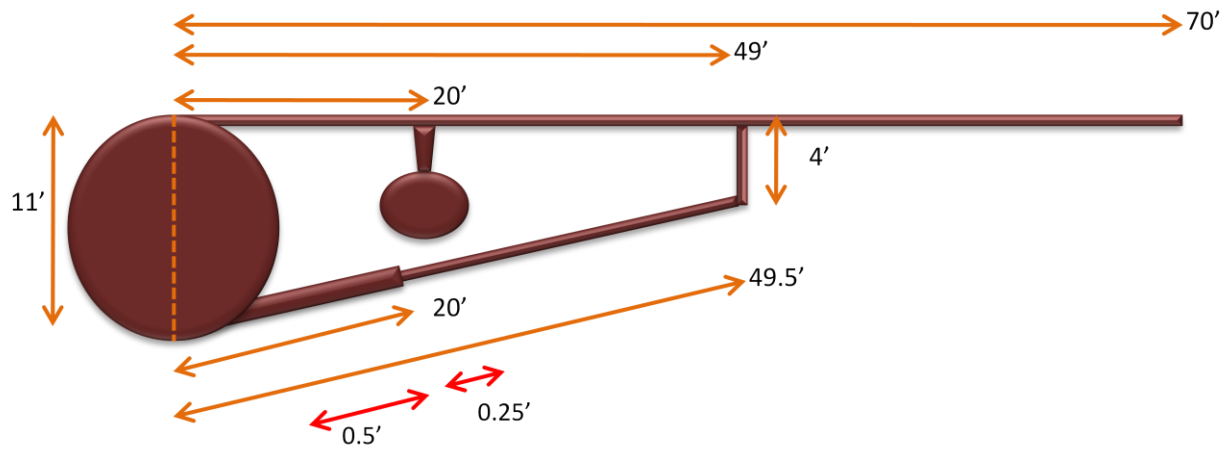

Figure 7.12 Design dimensions for the strut-braced wing (not to scale).

The red dimension lines indicate the “slack” for the negative and positive loads. A structural overview can be seen in Figure 7.13.

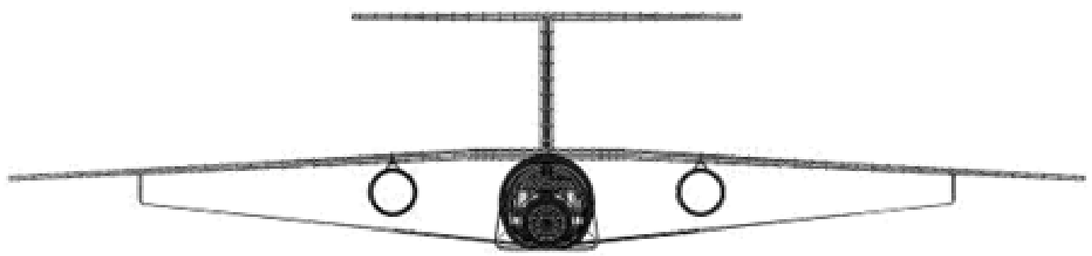

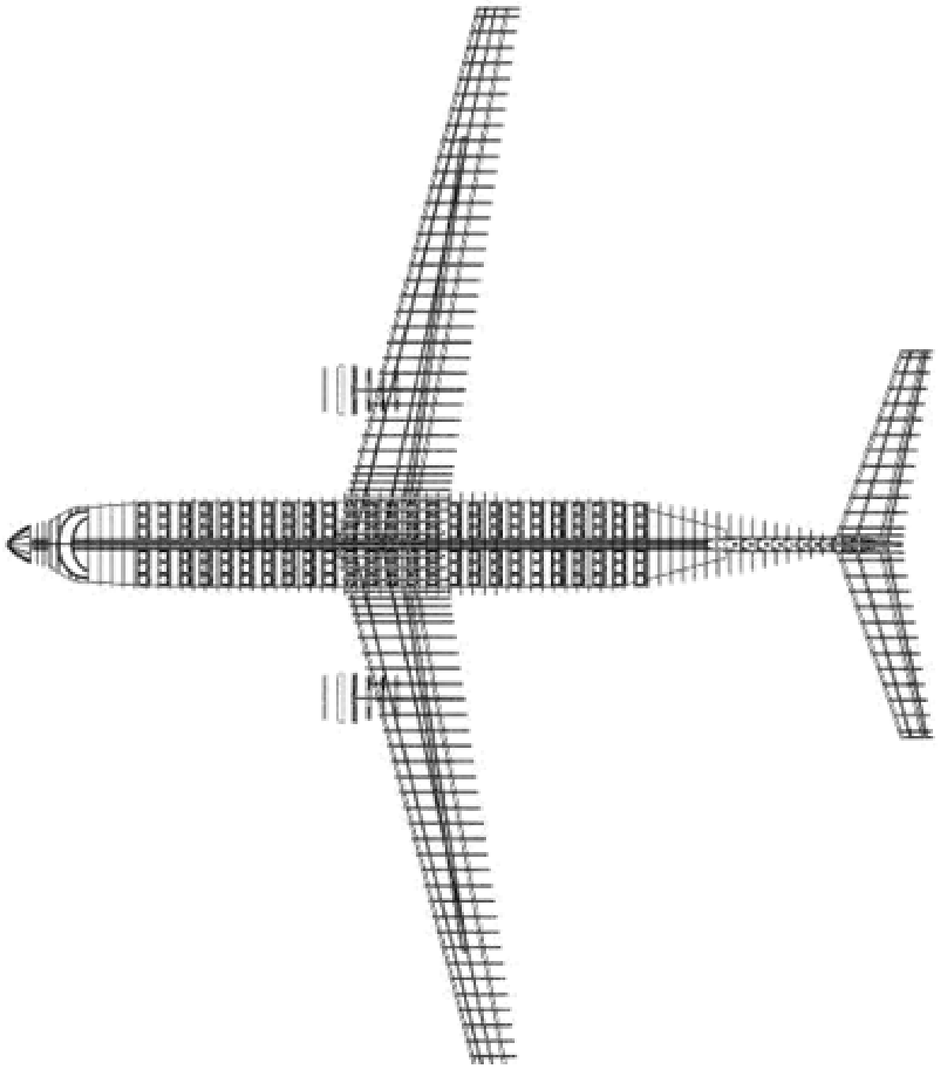

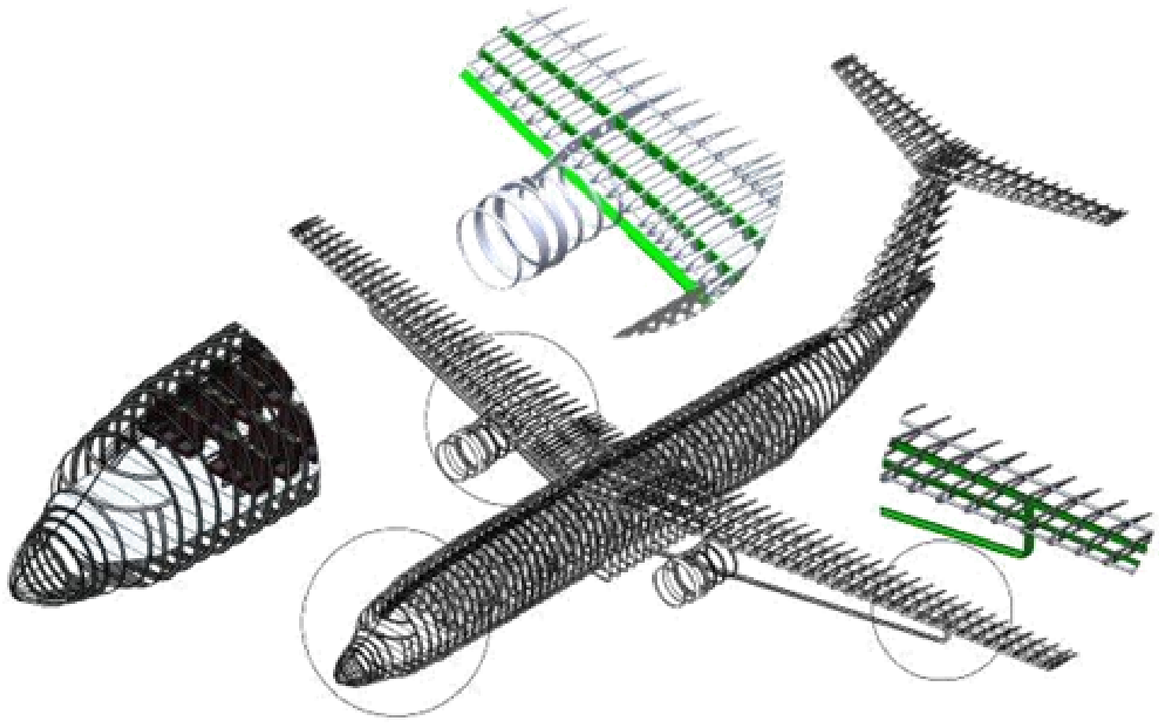

TITLE:

Structural Assembly

PROPRIETARY AND CONFIDENTIAL

THE INFORMATION CONTAINED IN THIS DRAWING IS THE SOLE PROPERTY OF <CF AERONAUTICS>. ANY REPRODUCTION IN PART OR AS A WHOLE WITHOUT THE WRITTEN PERMISSION OF

SIZE	DWG. NO.	REV
B		

Figure 7.13 Structural 3-view

8 Final Weights

8.1 Weight Components and CG Location

With the weights of the strut and wing finally calculated, weight component estimation for the entire aircraft can be determined. Raymer's text in Chapter 19 provides formulas for most of the components in a jet transport[8]. Roskam also provides weight component estimation and will also be used[23]. The weight component buildup will also provide an estimation location in inches for that component from the tip of the aircraft and the moment that it generates. If the location is indicated to be zero inches, then its affect on the CG is considered negligible. An average weight for the furnishings will be used since Roskam and Raymer's formulas have different results. The required payload of 37,000 lbs by the RFP and the 1,400 lbs crew will be assumed to be the 175 passengers, their luggage, and 7 crew members at 200 lbs each. If the average passenger weighs 170 lbs, the weight of luggage must be 7250 lbs. If this luggage is distributed in 2 main compartments and the fuel is estimated to be in 9 tanks (6 in wing, and 3 in fuselage) a CG for a full plane can be estimated for a 2200 nmi range.

To estimate the CG of a full aircraft, assumptions will need to be made for where the fuel and cargo will be placed within the aircraft. The first required estimation is how much fuel can be placed within the wing. A method of slicing the aircraft wing into sections as shown in Figure 8.1 will help provide this estimation:

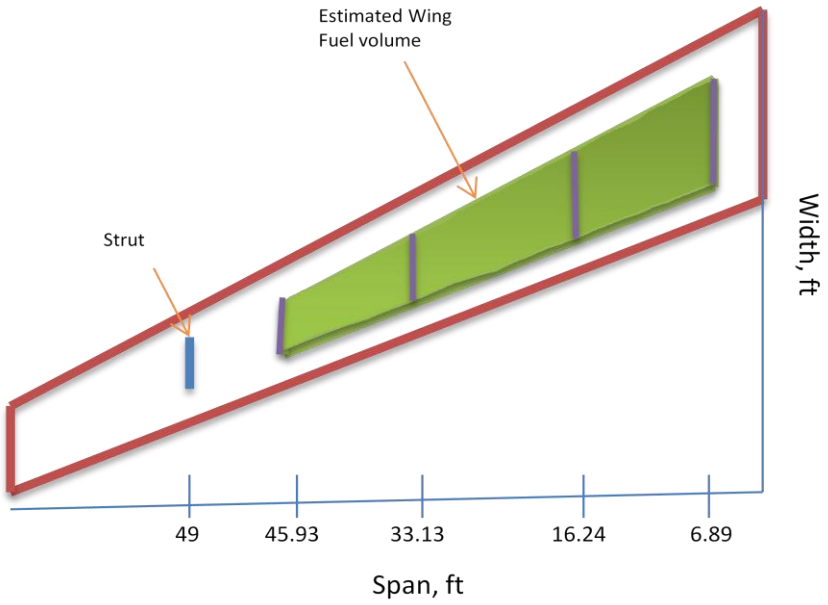

Figure 8.1 Visualization of wing fuel volume estimation

The green highlighted section of the wing represents where the fuel volume will be estimated. The estimated volume will be split into three sections as shown in Figure 8.2:

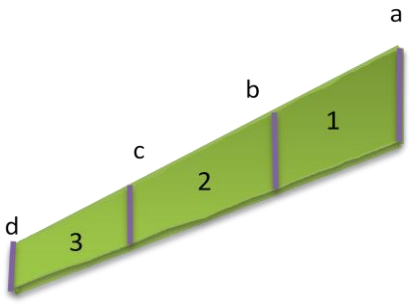

Figure 8.2 The wing fuel volume split into three sections.

At locations ‘a’, ‘b’, ‘c’ the chord, available thickness and span location will be found. For section ‘d’, the span location will only be needed. The volume at section 1 will be calculated by multiplying the chord, thickness, and length from ‘a’ to ‘b’, and respectively for sections 2 and 3. The thickness used in this estimation will be estimated by multiplying the chord by the t/c ratio of 10% and then subtracting the 2 times the plate thickness of the wing as calculated by the Van Hoek program. Once the total volume is found for all three sections (multiplied by 2 since the three sections was only for half the wing), this volume will be multiplied by 75% as recommended by Raymer[8]. The corrected volume will be multiplied by 7.5 since 7.5 gallons can occupy 1 ft^3 as provided by Raymer[8]. Finally, the density of JET-A at 0° F (6.7 lb/gal) will provide the total amount of fuel that be placed inside the wing. A summary of this weight component buildup is provided in Table 8.1.

Table 8.1 Weight Component Buildup

PLANETEER WEIGHTS SUMMARY					
Component	Weight	Xcg	Zcg	X-Moment	Z-Moment
	lbs.	in.	in.	lbs-in	lbs-in
Structures					
Wing	4901	606	210	2970006	1029210
Strut	1702	606	210	1031412	357420
Horizontal Tail	1159.3	1570	426	1820101	493861.8
Vertical Tail	1864.25	1491	318	2779596.8	592831.5
Fuselage	21365.31	649.5	144	13876769	3076604.6
Paint	498.62	0	0	0	0
Propulsion					
Engines	9000	582	190	5238000	1710000
Engine Nacelle Group	1703.84	582	190	991634.88	323729.6
Systems					
Main Landing Gear	3549.12	755	50	2679585.6	177456
Nose Landing Gear	904.48	161.88	50	146417.22	45224
Engine Controls	143.6	264	160	37910.4	22976
Starter (Pneumatic)	161.48	588	190	94950.24	30681.2
Fuel System	529.73	550	192	291351.5	101708.16
Flight Controls	2416.66	524	260	1266329.8	628331.6
APU installed	1837.5	1452	195	2668050	358312.5
Instruments	419.87	120	144	50384.4	60461.28
Anti-icing	284.92	576	210	164113.92	59833.2
Handling Gear	42.74	996	120	42569.04	5128.8
Air Conditioning	1340.92	921	204	1234987.3	273547.68
Hydraulics	347.65	342	204	118896.3	70920.6
Electrical	942.78	546	160	514757.88	150844.8
Avionics	1032.64	36	150	37175.04	154896
Oxygen System	151.3	921	144	139347.3	21787.2
Furnishings					
Misc. (Galleys, restrooms)	2097.685	921	144	1931967.9	302066.64
Seats	3617.25	921	144	3331487.3	520884
Fuel					
Wing Fuel Tanks	11765.86	606	210	7130108.8	2470829.8
Fuselage Tank 1	6400.05	618	108	3955229.7	691205.18
Fuselage Tank 2	6400.05	582	108	3724827.9	691205.18
Fuselage Tank 3	6400.05	570	108	3648027.3	691205.18
Payload					
Pilots and Crew	1400	816	144	1142400	201600
Passengers	29750	921	144	27399750	4284000
Luggage Comp 1	3625.00	726	108	2631750	391500
Luggage Comp 2	3625.00	486	108	1761750	391500
TOGW	131380.65			94851644	12798105
Zero fuel with Payload	100414.645			76393451	15837317
Empty Weight	62014.645			43457801	10568717

	X-CG (ft)	Z-CG (ft)
TOGW	60.16	8.12
Zero fuel with Payload	63.40	13.14
Empty Weight	58.40	14.20

9 Aircraft Performance

In order to comply with the AIAA 2010 RFP, the Planeteer had to meet the performance requirements discussed in the introduction. These specifications included a takeoff field length no greater than 8200 feet at sea level, a maximum landing speed of 140 knots, a maximum range of 3500 nautical miles, and a cruise speed of Mach 0.8 at 35,000 feet or greater.

9.1 Takeoff Distance

One of the key performance requirements specified in the RFP is takeoff distance, which is required to be less than 8200 ft. Using a method developed by Anderson[24], basic takeoff distance was calculated as a function of both density altitude and gross takeoff weight, with the resulting contours plotted in Figure 9.1 below. Note that the gross takeoff weight is approximately 136500 lb, which is less than the RFP requirement up to a density altitude in excess of 9000 ft. This suggests acceptable "hot-and-high" performance. The engine deck used is a GE-90 class high-bypass turbofan engine, which is likely typical of a modern, high-bypass turbofan engine. The engine deck was used by John Gundlach in his Masters thesis, and is based on work by Mattingly[25].

$$\frac{T}{T_{SL,static}} = (0.6069 + 0.5344 \cdot (0.9001 - M)^{2.7981}) \cdot \left(\frac{\rho}{\rho_{SL}}\right)^{0.8852} \tag{9.1}$$

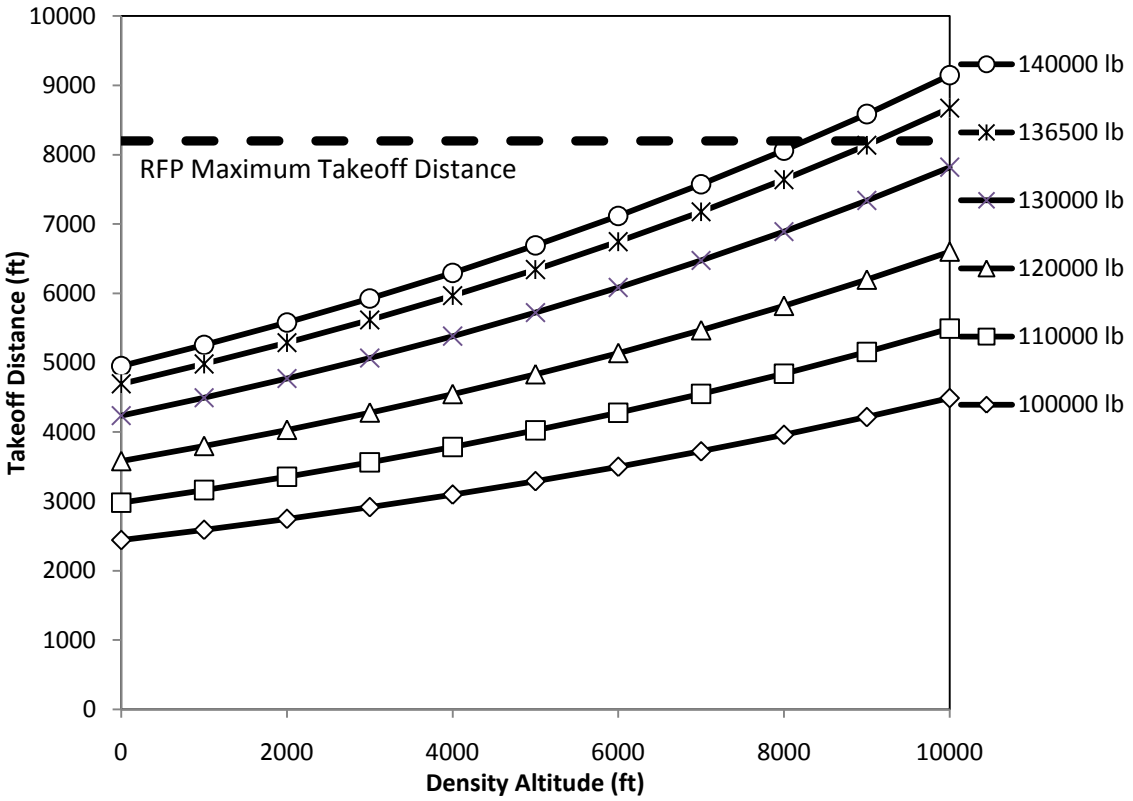

Figure 9.1 Takeoff Distance vs. Takeoff Weight and Density Altitude

9.2 Best Cruise Altitude (BCA) / Best Cruise Mach (BCM)

Usually the purpose of constructing a set of curves for BCA/BCM is to determine both entities, however, BCM has already predetermined in the RFP to Mach 0.8. Therefore, the goal is to find the BCA for the optimal specific range of the aircraft. It is also important to factor in the drag rise to each altitude curve. The resulting equation for specific range is,

$$sr = \frac{M_\infty a}{sfc} \frac{C_L}{C_D} \frac{1}{W} \tag{9.2}$$

where a is the speed of sound, sfc is the specific fuel consumption and W is the overall weight of the aircraft[15]. By varying Mach, the ensuing figure is produced.

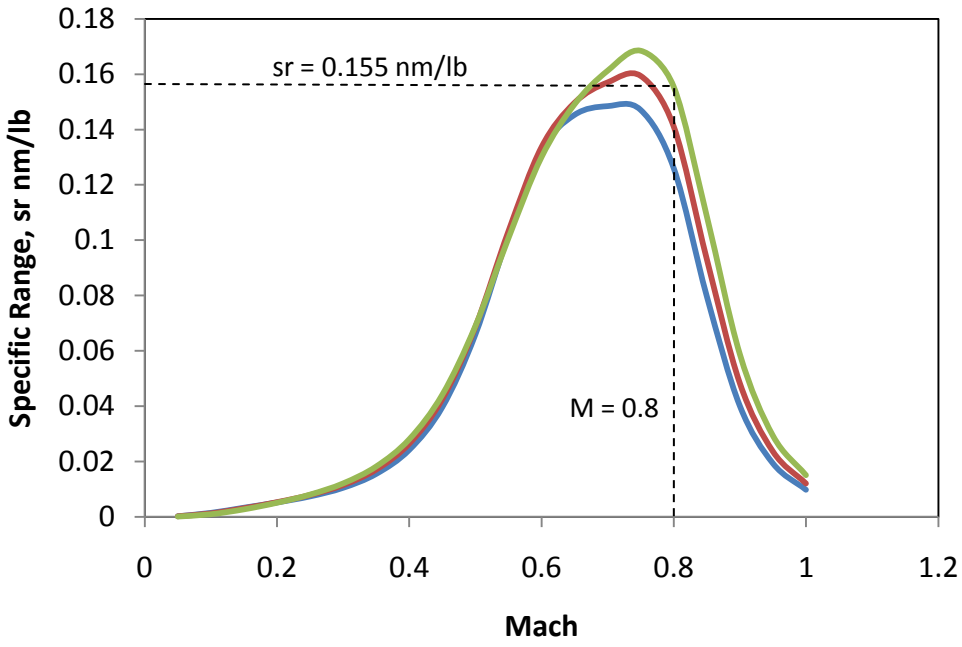

Figure 9.2 Specific range with varying Mach number for multiple altitudes.

Based on Figure 9.2, the optimal specific range at M=0.8 is 0.155 nm/lb while flying at a BCA of 40,000 feet. Taking into account the total fuel capacity of the Planeteer, the maximum specific range is about 4,800 feet.

9.3 Mission Performance

To verify that the Planeteer is capable of performing the design mission included in the RFP, a simulation of the mission was run using a MATLAB code originally developed by Mike Morrow at Virginia Tech[26]. For the purposes of this simulation, descent times are included in the subsequent loiter times. This mission is roughly a 1200 nm flight at 40,000 ft and Mach 0.8, and includes allowances for taxi, takeoff, climb, cruise, an attempted landing at the primary airport, a go-around, diversion to an airport 200 nm away, landing, and taxi to the gate. As Table 9.1 shows, the Planeteer is capable of flying this mission with additional fuel reserves remaining after the diversion to an alternate airport. Note the program steps through each mission segment in parts; only the final part data is shown in the table.

Table 9.1 Mission for the Planeteer

Mission Segment	Time (min)	Mach	TAS (knots)	Altitude (ft)	Fuel Remaining (lb)	Distance (nm)
1. Warm-up, taxi	15	0.00	0	0	24819	0
2. Takeoff	17	0.00	0	0	24301	0
3. Climb to 10000 ft at best rate of climb	19	0.53	339	10000	23700	13
4. Climb to 40000 ft at best economy climb	49	0.68	392	40000	20825	197
5. Cruise for 1200 nm at M=0.8	206	0.80	459	40000	10390	1397
6. Descend to 10000 ft	-	-	-	-	-	-
7. Loiter for 20 minutes	226	0.29	182	10000	9583	1458
8. Go around- full thrust for 2 minutes	228	0.29	0	10000	9223	1397
9. Cruise for best economy at 10000 ft for 200 nm	281	0.35	225	10000	6833	1597
10. Loiter for 20 minutes	301	0.28	179	10000	6055	1657
11. Descend to sea level	-	-	-	-	-	-
12. Idle thrust for 15 minutes	316	0.28	0	0	2142	1597

10 Stability and Control

The goal set forth by CP Aeronautics was to design an aircraft that meets the stability and control requirements set forth by the FAR, MIL-STD[1] and the AIAA supplied RFP. In order to accomplish this goal, the CP-01 was designed with traditional control surfaces and tail sizes set to meet engine out flight requirements as well as nose pitching up moment for lift off and flight. Control surface sizing, neutral point location determination, static and dynamic analysis was all determined using a plethora of programs and methods of analysis. The programs used for these calculations included LDstab (Lateral Direction Stability)[2], VPI-NASA Excel spreadsheet, and Tornado VLM (Vortex Lattice Method)[3]. The Tornado program was used to calculate location of the neutral point by finding the static margin and the stability derivatives. LDstab (Lateral Directional Stability)[2] was used to determine the engine out criteria as well as to find the stability derivatives.

10.1 Horizontal Tail

The horizontal tail on the Planeteer was sized to meet the neutral point requirements as well as nose up pitching requirements. The apex of the horizontal tail is located at the front of the tip of the vertical tail. The horizontal tail is kept out of the wake of main wing by use of a T-tail configuration which places the horizontal tail 18 feet about the main wing. This is done to increase the effectiveness of the horizontal tail by keeping its flow free of turbulence created by the main wing. Interference from the main wing does not occur until the freestream angle of attack exceeds 15 degrees. The horizontal tail, show in Figure 10.1 below, is dimensioned to have a 50 foot wingspan, a root chord of 9 feet, a tip chord of 4 feet, a reference area of 334 square feet.

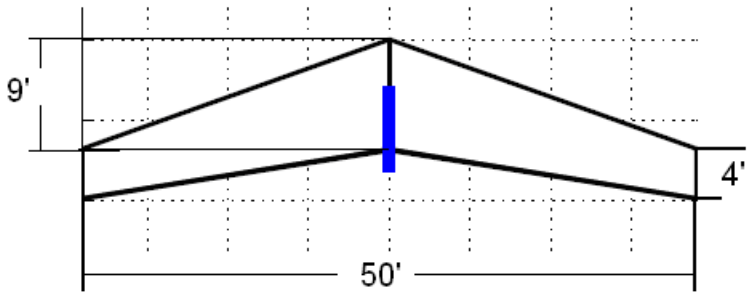

Figure 10.1 Horizontal Tail Geometry

10.2 Vertical Tail

The vertical tail for the Planeteer was designed to supply a sufficient yawing moment coefficient as determined by the engine out condition. In addition, cross wind analysis was performed to ensure sufficient sizing of the wing. The vertical tail is 18 feet tall, has a root chord of 18 feet, a tip chord of 9 feet to match the root chord of the horizontal tail, and a reference area of 236 square feet. The root chord of the vertical tail sits atop the fuselage at the same vertical station as the main wing. The aspect ratio for the vertical tail is 1.37 and it is appropriately sized to meet engine out and cross wind conditions.

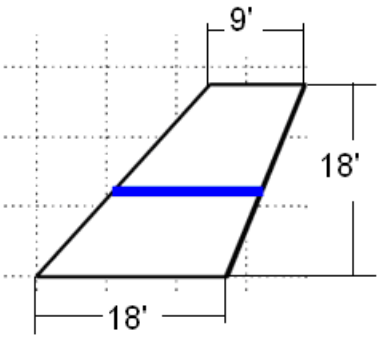

Figure 10.2 Vertical Tail Geometry

Engine out analysis for the vertical tail was done using the LDstab (Lateral Directional Stability)[2] program. The basic requirement for this code is that the available yawing moment coefficient is greater than the required yawing moment coefficient created by a single engine out scenario. The required yawing moment coefficient is determined by the drag created by the inoperative engine and the contributions of windmilling effects. Under FAR 25.149, supplied by Roskam[1], the aircraft must be able to meet or exceed the required yawing moment coefficient for steady flight at a speed $1.2V_{stall}$ with one engine inoperative. The other engine must maintain maximum thrust (~23,000lbs for the Planeteer) while not exceeding a bank angle of 5 degrees. The required yawing moment coefficient was calculated using the method described by Torenbeek by taking into account the drag due to windmilling of the failed engine. Table 10.1 below shows the results supplied by the LDstab (Lateral Directional Stability)[2] program as well as the calculated required yawing moment coefficient $Cn_{required.}$ It can be seen from the results that the aircraft is able to meet the required yawing moment coefficient while maintaining a bank angle of 5 degrees and only experiencing a 1.62 degree sideslip angle and a 1.28 degree aileron deflection.

Table 10.1 Engine out Analysis

Variable	Results
β	1.62
φ	5
δa	1.28
δr	20
Cn_{avail}	0.030
Cn_{req}	0.0050

10.3 Neutral Point

The neutral point was for the Planeteer was found using Tornado's VLM[3]. The aircraft surfaces that interact with the stability of the aircraft were modeled as flat surfaces made up of numerous panels. The body of the aircraft was modeled by using 10 chordwise and 10 spanwise panels in a mesh and was located at the fuselage vertical centerline. The main wing was modeled by a mesh of 10 chordwise and spanwise panels while the control surfaces were modeled by a mesh of 5 chordwise and spanwise panels. The vertical and horizontal tail were also modeled by use of a mesh consisting of 10 chordwise and spanwise panels with the control surface modeled the similarly to the main wing. A model of the aircraft geometry used for calculations in the Tornado's VLM[3] program is shown in Figure 10.3 below with the location of MAC and CG shown. The Planeteer is designed so that the neutral point is located at 44.7% of the MAC with a static margin ranging between approximately 15 and 8.5% depending on aircraft loading. This CG travel is shown in Figure 10.4 below between the upper and lower limits of static margin. A low static margin, also known as tail heavy, leads to less stability but greater elevator effectiveness. On the other hand a high static margin, known as nose heavy, creates a more stable aircraft but limits the elevator effectiveness. This static margin, between 5 and 15%, makes the CP-01 a stable aircraft in all phases of flight. As fuel is consumed the CG of the aircraft moves forward, thus the static margin is designed to be between 5 - 15% through all phases of flight.

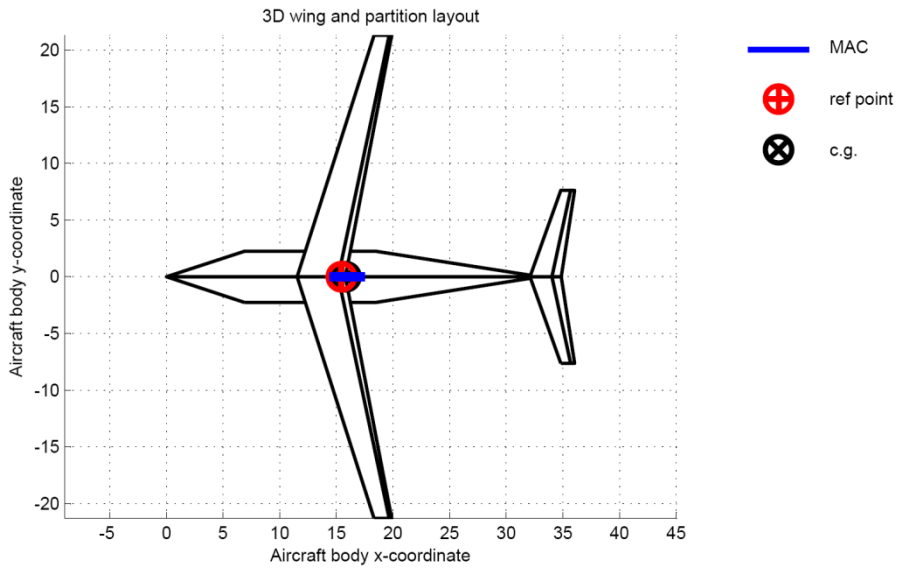

Figure 10.3 Tornado VLM Geometry

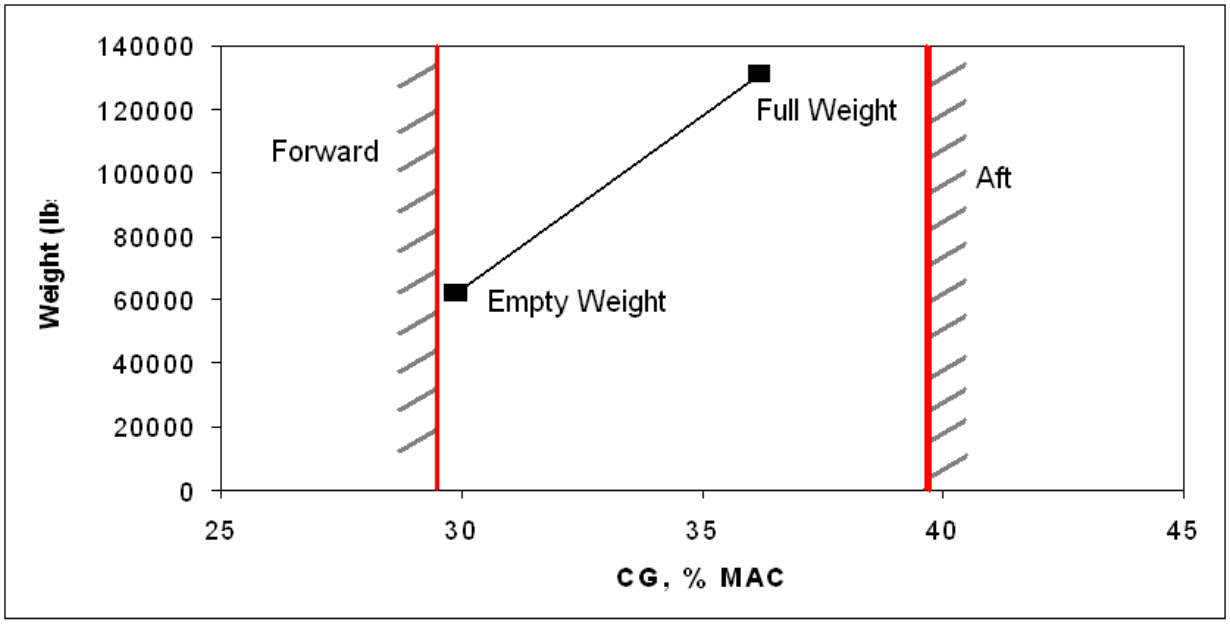

Figure 10.4 Static Margin with Change in CG Location

10.4 Control Surfaces

The Planeteer is designed to meet all in flight maneuvering requirements. This section details the rudder, elevators, and ailerons and the reason for their use in flight.

The rudder was sized to fulfill the engine out criteria which was shown in the results of the LDstab (Lateral Directional Stability)[2] program. The control surface, as common with current convention, is divided into two

separate sections. The sections can deflect together in the case of low speed conditions, or only the bottom rudder will deflect in the case of high speed conditions. The reason for this is because at higher speeds less lifting surface is required to create the required moment for yawing. To meet the required yawing moments the rudder was sized to be 35% of the chord of the vertical tail while spanning 14 feet to give it a surface area of 66.15 feet squared. The rudder span was sized to not interfere with the horizontal tail elevator deflections.

The elevators were sized in order to supply the aircraft with the necessary pitching moment needed for trimmed flight. The elevators span 22 feet of each side of the horizontal tail as to not interfere with rudder deflections. The elevators were sized to be 30% of the horizontal tail chord giving the elevators a total surface area of 85.8 square feet.

The ailerons were sized to meet two requirements. First being roll performance as outlined in MIL-F8785 in the appendix of Roskam[1] while also being able to maintain proper trimmed flight during an engine out event. According the MIL-F875B the aircraft must be able to roll 30 degrees in 1.5 seconds in order to meet Level 1 standards for a Category B Class III aircraft. In order to determine the sizing of the ailerons methods from Etkin and Reid[5], VPI-NASA spreadsheet and the stability derivatives calculated for the engine out case were used. These results yielded the ailerons to be sized to a value of 30 % of the wing chord with a span of 8 feet each. This geometry gives a required aileron area of 73 feet with each aileron being placed span wise at a location to ensure maximum moment arm. With this aileron geometry, the CP-01 can roll 45 degrees in 1.5 seconds and only requires 1.2 seconds to roll the required 30 degrees. These results are shown in Figure 10.5 below.

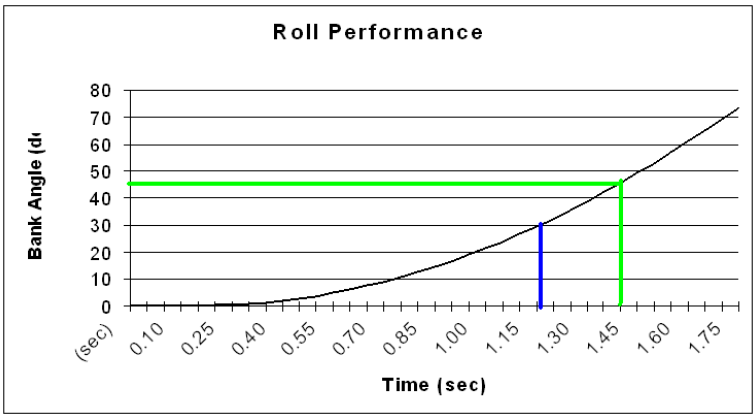

Figure 10.5 CP-01 Roll Performance Results

Table 10.2 Stability and Control Derivatives

Stability and Control Derivatives	Value		Stability and Control Derivatives	Value
Cl_β	0.004069		Cy_{da}	-0.582
Cl_p	-0.61425		Cl_{da}	0.6532
Cl_r	0.090077		Cn_{da}	-0.233
Cn_β	-0.18119			
Cn_p	0.044849		Cy_{de}	0.019382
Cn_r	-0.13896		Cl_{de}	-0.00295
Cy_β	-0.54551		Cn_{de}	0.007848
Cy_p	-0.02118			
Cy_r	-0.38973		Cy_{dr}	-0.23839
			Cl_{dr}	0.025867
			Cn_{dr}	-0.10563

10.5 Dynamic Analysis

For the dynamic analysis of the Planeteer, methods from Etkin and Reid[5] were used once again as well as the results from the LDstab (Lateral Directional Stability)[2] code. Due to the lack of specific dynamic flight requirements outline in FAR part 25, MIL STD Class III Category B requirements found in Roskam[1] were used to determine if the dynamic response of the aircraft was within acceptable limits. Table 10.3 below shows the dynamic response requirements set forth by MIL STD as well as the current dynamic response characteristics of the CP Planeteer. The Short Period mode is heavily affected by the pitch stiffness and pitch damping of the aircraft, which in large part are determined by the horizontal tail volume. The phugoid mode on the other hand is more heavily influenced by the speed and the lift to drag of the aircraft. As seen in the chart below, the CP-01 has a pretty high natural frequency in the short period mode with a somewhat low damping. While the response characteristics are within the acceptable limits, flight control systems will be used to assist the pilots in order to make the aircraft feel more stable in flight.

Table 10.3 Planeteer Dynamic Characteristics

		MIL-STD Cat. B Level 1 Class II	Planeteer
Phugoid	Damping	$\zeta_p > 0.04$	0.41595
Short Period	Damping	$0.3 < \zeta_{sp} < 2.0$	0.33
	Natural Frequency (rad/sec)	$0.8 < \omega_{sp} < 1.9$	1.65

11 Aircraft Systems

To compete with aircraft in the 2020s, the Planeteer design incorporates a wide variety of advanced technologies throughout all of its systems.

11.1 Electrical Systems

The Planeteer utilizes a no-bleed architecture for its electrical system. Rather than using engine-generated pneumatics to power functions such as air-conditioning and wing de-icing systems, electrical power produced by generators are used. The major advantage of a no-bleed system is the greater efficiency gained in terms of reduced fuel burn. The new Boeing 787 utilizes this type of architecture and Boeing predicts fuel savings of about 3 percent over traditional systems[50].

An APU is used to provide the power necessary to start the twin PW1000G engines without additional support from ground units. It can also provide back-up electrical power in the event of a main engine power failure. A lead acid battery is used to provide DC power to start the APU and provide in-flight emergency power in case the APU needs to be restarted. A generator in each engine is used to provide primary electrical power to the various aircraft systems in flight. A wind-turbine generator is also installed to provide power to the flight control system in the event of a complete engine and APU failure during flight. The combination of these back-up systems with the no-bleed architecture ensures that the electrically-based flight controls will remain operational during every flight condition.

11.2 Flight Control Systems

The hydraulic system in the Planeteer's no-bleed architecture is similar to that of traditional architecture aircraft. Three independent systems are used to collectively support primary flight control actuators, landing gear actuation, nose gear steering, thrust reversers, and flaps. The systems are located in the left, center, and right of the aircraft. The left and right systems are driven by engine-mounted pumps on the engine gearbox. For peak demands and ground operations, the left and right systems are additionally powered by an electrically driven pump. The center system is powered by two large electrically driven pumps. One of the pumps operates for the entirety of the flight while the other pump only runs during takeoff and landing. The pumps in the Planeteer maintain a higher pressure than those in a traditional system which enables the airplane to use smaller hydraulic components, saving

both space and weight. A hydraulic system is used rather than electro-mechanic because the composite wing structure would have trouble dissipating the heat generated by electro-mechanic actuators.

To deflect control surfaces on the Planeteer, hydraulically driven actuators are used. Linear actuators control the primary flight controls, specifically the deflection of ailerons, elevators, rudders, and spoilers. Rotary actuators are used for secondary flight controls to extend and retract the flaps.

The entire flight control system is electronically controlled by fly-by-light technology. The advantages this has over fly-by-wire are higher data transfer speeds and immunity to electromagnetic interference.

To account for the stability characteristics of the Planeteer and to make flying as easy as possible for pilots, a flight control computer is used to interpret inputs from the pilot and send the intended command to each control surface. This allows the Planeteer to remain as safe as possible during flight while remaining responsive to pilots

11.3 Flight Deck Systems

The Planeteer flight deck follows the configuration of the newest commercial aircraft, the Boeing 787. It is similar to those of the Boeing 737NG and Airbus A320 with the addition of a heads-up display (HUD) system for both the pilot and co-pilot to allow current 737 and A320 pilots to easily make the transition to the Planeteer[32].

The glass cockpit display is made up of four 8 by 10 inch liquid crystal displays as well as an additional 10 by 13 inch display in the center control console. It is designed to provide superior display space but require fewer displays than current aircraft.

The control yoke is identical to the one in the Boeing 737NG. This allows 737 pilots to make an easy switch to the Planeteer. A yoke is used rather than a simpler side-stick in order to make the transition for current 737 pilots as smooth as possible.

The HUD is a new feature in commercial aviation cockpits. Like in military aircraft, the HUD provides flight data to the pilots on a piece of glass in front of them so they do not have to look down on the display panels. The use of a HUD and glass cockpit ensures that the Planeteer remains competitive yet familiar.

A mockup of the Planeteer flight deck can be seen in Figure 11.1 below.

Flight Deck Components

1 - Overhead Panel
2 - Heads-up Display
3 - Autopilot Control Panel
4 - Primary Flight Display
5 - Navigational Display
6 - Auxiliary Display Panel
7 - Throttle

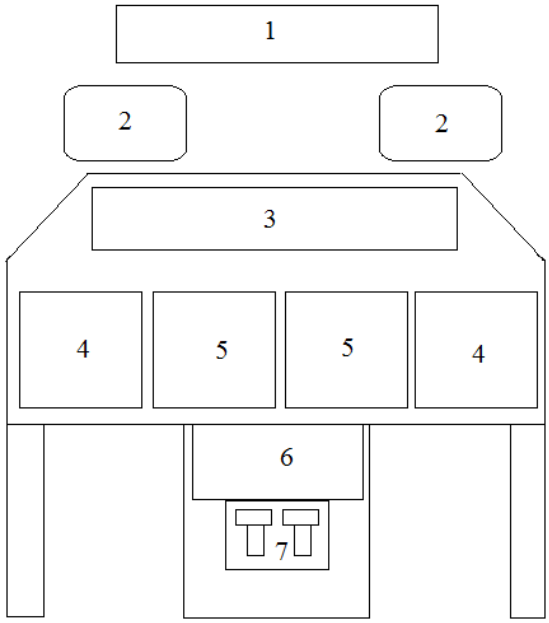

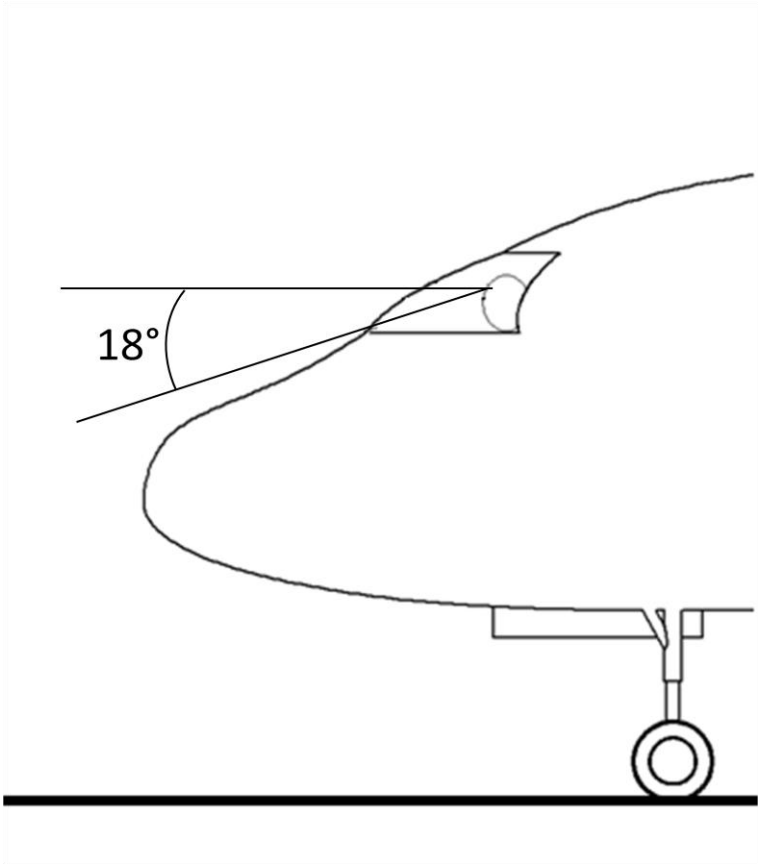

Figure 11.1 Flight Deck Layout

11.4 Cabin Systems

The cabin layout of the Planeteer is nearly identical to that of the Boeing 737-800. It is a single aisle configuration with 175 seats. The seats have a width of 17.2" and pitch of 32". Each seat has a personal entertainment system powered by a module under the seat. The Planeteer has three lavatories, one fore and two aft. There are two galleys, one fore and one aft. There are emergency exits on both port and starboard sides at the fore and aft of the cabin and under the wing. They are equipped with inflatable slides to allow quick exit in an emergency. The overall layout of the cabin can be seen in Figure 11.2.

During flight the cabin will be pressurized to 12.2 psi, equivalent to an altitude of 5,000 ft.

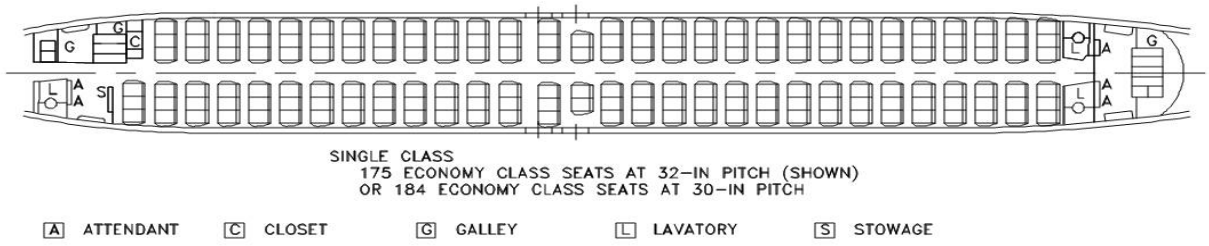

Figure 11.2 Cabin layout[10].

11.5 Fuel System

The Planeteer features nine fuel tanks. Three tanks are located in the cargo compartment under the wing and are made from aluminum alloy. In addition, each wing contains three bladder-style tanks. They are located between the front and rear wing spars. Table 11.1 contains the total fuel volume and weight for both the wing and fuselage tanks. Nitrogen is used to replace spent fuel in the tanks to prevent an explosion during flight.

Table 11.1 Fuel Tank Sizing.

	Total	**Wing**	**Fuselage**
Fuel Weight (lbs)	30966	11765.86	19200.14
Fuel Volume (gal)	4621.79	1756.10	2865.59
Fuel Volume (ft^3)	616.24	234.15	382.10

11.6 Landing Gear

The Planeteer uses a tricycle landing gear configuration to ensure that the aircraft can utilize existing loading technologies at current airports. The main gear consists of four wheels positioned aft of the center of gravity

at 15° from the vertical. The nose gear consists of two wheels. The Planeteer has a wheel track of 18.5 feet, with a turn-over angle of 54° and a tail-strike angle of 11°.

Unlike a conventional design, the Planeteer has a high wing making it difficult to integrate the landing gear. In order to meet turn-over requirements the wheel track must be wider than the fuselage. To meet this requirement there are two fairings smoothly attached to the fuselage under the wing from which the main landing gear extend.

The wheels are sized according to Raymer's[8] guidelines and produce the following results. The main gear wheels are 44.5 inches in diameter and 14.5 inches wide. The nose gear wheels are 27 inches in diameter and 7.75 inches wide. A drawing of the landing gear can be seen in Figure 11.3.

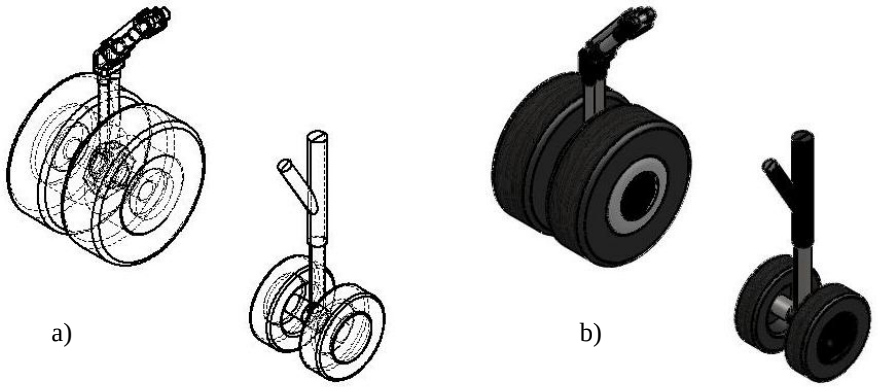

Figure 11.3 Nose and Main Landing Gear

11.7 Lighting System

The Planeteer features a high performance exterior lighting system which is federally mandated by the FAA. Rather than conventional halogen bulbs, LEDs are used because they are more reliable and have an extended lifespan. The lighting system is configured as displayed below in Figure 11.4.

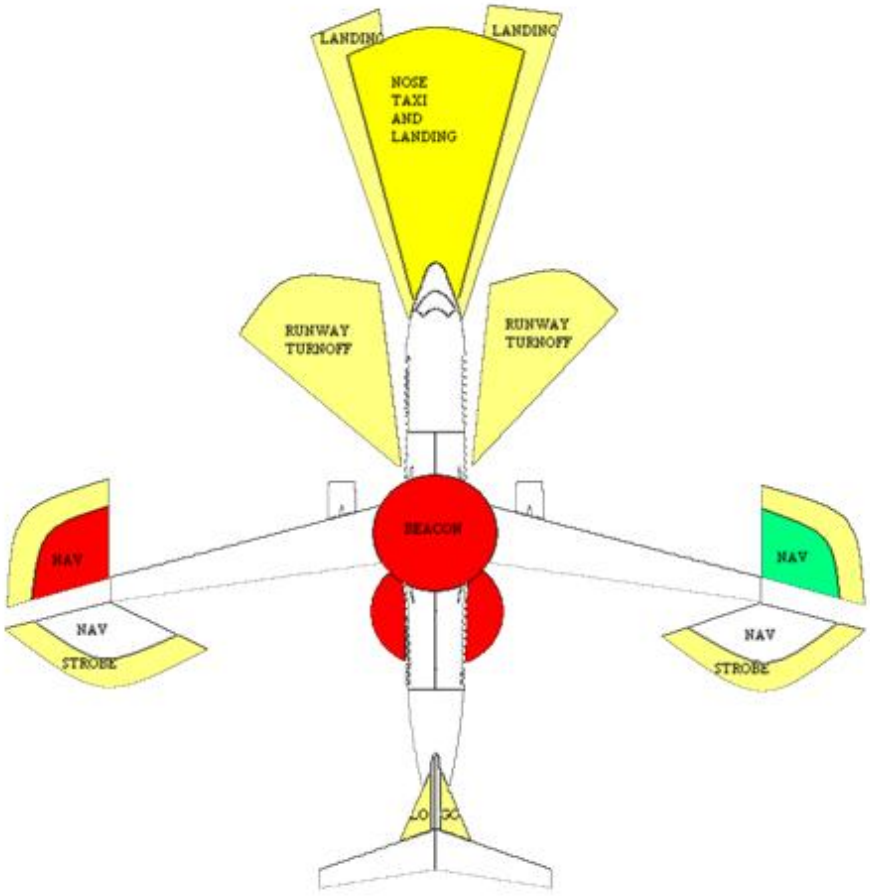

Figure 11.4 Exterior light configuration.

11.8 De-icing System

The Planeteer features a new heating system designed by GKN Aerospace. Rather than using bleed air to de-ice the control surfaces of the wing, several heating mats formed through multiple layers of composites are used. This new system is currently being installed on the Boeing 787. The heating element is integrated into the composite wing using a sprayable conductive layer. This system requires minimal electricity and the absence of bleed air removes the noise associated with the de-icing process[35].

12 Ground Systems

In order to comply with the 2010 AIAA RFP, the entire aircraft system, including those on the ground, must be considered for the Planeteer.

12.1 Airport Gate Sizing

In Advisory Circular (AC) number 150/5300-13, the Federal Aviation Administration offers regulatory guidance on the design of airports. This includes defining six "design groups" to categorize aircraft based on their external dimensions. This is used particularly in airport design in sizing the airport gates. These definitions are summarized in Table 12.1, which is copied from change 10 to the above AC.[36]

Table 12.1 Airplane Design Groups (ADG)[36]

Group #	Tail Height (ft)	Wingspan (ft)
I	<20	<49
II	20 - <30	49 - <79
III	30 - <45	79 - <118
IV	45 - <60	118 - <171
V	60 - <66	171 - <214
VI	66 - <80	214 - <262

Both the Airbus A320 and the Boeing 737 families, which constitute nearly all aircraft in this class, meet the definition for Group III. However, the Planeteer fits into the next group, Group IV. The improvement in fuel efficiency will adequately offset the added expense to airports and airlines to use larger gates or modify existing gates and terminals for new aircraft.

12.2 Alternative Fuels

Once referred to as moonshine by an ExxonMobil executive[37], biofuels have been brought to the forefront of the effort to reduce our national oil consumption. Biofuels are fuels derived from plant matter that can replace existing fossil fuels. The "holy grail" is to create a fuel that generates the same energy as petroleum-based fuels, such as Jet-A, is inexpensive, and is environmentally friendly.

Biofuels are considered to be nearly carbon neutral, meaning no net carbon is added to the atmosphere through their burning. The idea behind this is that the plants from which biofuels are made absorb large amounts of

carbon dioxide, CO_2, from the atmosphere when growing. When the plants are converted into fuel and later combusted, this CO_2 is then released back into the atmosphere making a zero net impact on the atmosphere. In contrast, fossil fuels, which would otherwise be trapped below the earth's crust, release large amounts of CO_2 into the atmosphere. Unlike biofuels, fossil fuels don't absorb any CO_2 during their lifecycle therefore resulting in a net increase in the amount of carbon dioxide in the atmosphere.

CP Aeronautics carefully considered a wide range of biofuels to use in this study per the RFP guidelines. These included first generation biofuels such as vegetable oil and ethanol from sugar cane as well as second generation biofuels like ethanol derived from cellulous. The most important requirements for choosing the best biofuel to use were energy content, the feasibility of mass production, and compatibility with the broad range of environments and airliners. Biofuel made from algae, also known as algae fuel, was chosen as the best option following substantial research. The chemical properties of this biofuel are very similar to that of Jet-A; so similar in fact that a recent paper published by the United States Air Force regarding the use of algae fuel shows the chemical properties of algae fuel as nearly identical to those of Jet-A[38]. The specific chemical composition of algae fuel and other alternative fuels is summarized in Table 12.2.

Table 12.2 Algae fuel chemical composition.[38]

Fuel	Specific Energy MJ/kg	Energy Density MJ/I	Boiling Point °C	Freezing Point °C	Viscosity at 40°C
Jet Fuel	43.2	34.9	150-300	<-40	1.2
Algae Jet Fuel	#	#	#	#	#
Biodiesel	38.9	33.9	>400	0	4.7
Ethanol	27.2	21.6	78	-183	1.52
Butanol	36	29.2	118	-89	3.64

Algae jet fuel properties similar to jet fuel

These properties, including freezing point, are comparable to those of Jet-A. With other biofuels, a major concern in their use in commercial aviation is the fact that they freeze at a higher temperature than Jet-A, necessitating heating at high altitude or in cold weather to prevent freezing. With algae fuel, this problem can be eliminated at the refinery. Algae fuel can be refined in such a way that its freezing point is comparable to that of Jet-A. Also, it is important to note is that the density of algae fuel at 15^0C is 804 kg/m^3 which is similar to that of Jet-A. This means that when sitting on the ramp, an aircraft's tanks can still hold the same amount of algae fuel as jet fuel.

Algae fuel currently costs approximately $20/gallon. While this value may seem alarming, this is due to the small quantities currently produced; mass production is expected to drop prices to $3 per gallon or less[38]. Algae create 30 times more energy per unit area of land than previous generation biofuels (i.e. 1 acre of algae can produce the same energy as 30 acres of ethanol grown from sugar cane). To power the entire US, an area just $1/7^{th}$ that of the land currently being used to cultivate corn would need to be dedicated to algae growth. This land area would amount to roughly the size of the state of Maryland. Simplifying this task is the fact that algae can be grown anywhere including freshwater, saltwater, and even in indoor habitats provided sunlight is allowed to enter. Swampland, which may be otherwise unusable, may be an ideal area to grow and cultivate algae. Using this logic, it is reasonable to assume that algae fuel can be mass produced without significantly impacting food prices as previous biofuels did.

In addition to having the same chemical properties of Jet-A and being suitable for mass production, algae fuel is also a drop-in fuel. This results in minimal changes to existing airport infrastructure. Current and planned jet engines will be able to run algae fuel without needing modifications, and the fuel lines supplying the fuel within the aircraft would also not be affected. Similarly, fuel trucks, fuel hoses, and underground fuel tanks at airports around the world would also be suitable for immediate use with algae fuel without costly upgrades or replacements.

Several major aviation companies have already begun testing biofuel in their aircraft. The table below summarizes recent events.

Table 12.3 Biofuel Flights Accomplished[39,40,41,42].

Organization	Date	Equip.	Blend	Results
US Air Force	Mar 10	A-10	50-50 Biofuel/JP-8	First ever flight flown solely on biofuel blend
Continental Airlines	Jan 09	B737	50-50 Algae Fuel/Jet-A	Airline quoted as saying Algae Fuel *outperformed* Jet-A
Air New Zealand	Jun 09	B747	50-50 Jatropha/Jet-A	2,000 lbs of Jet-A saved; CO_2 emissions cut by 60%
KLM	Nov 09	B747	50-50 Camelina/Jet-A	First airline flight with passengers aboard

Industry has clearly embraced the idea of using biofuel blends to cut down on fossil fuel usage and CO_2 emissions. In March 2010, Airbus parent company EADS furthered the push for use of biofuel when their Chief Technical Officer, Jean Botti, went on the record saying, "We absolutely need to push third-generation biofuels made from algae[43]." He goes on to say that any CO_2 produced in the algae fuel production process could be sequestered and pumped back into the algae's growing environment making it a truly carbon-neutral process. Botti

also notes that EADS is the spearhead of the algae fuel mission and that they are working in aligning the rest of the industry with the vision for the future of algae fuel.

As evidenced by flight tests, algae fuel is the most promising biofuel. The Planeteer uses a drop-in algae fuel as its fuel of choice.

12.3 NextGen

By the year 2020, when the Planeteer is scheduled to enter service, the FAA's NextGen initiative will be in use across North America[44]. This project, already underway, revolves around the FAA's plan to replace current air traffic control methods with new ways to control air traffic. The idea is to replace ground based radar stations with satellite technology to track and communicate with aircraft in flight. The only change in equipment required of the airframe manufacturer is an updated transponder, a piece of hardware currently in every transport aircraft. A transponder is what allows an aircraft to be seen on radar and transmit to the radar station various parameters such as altitude and heading.

This new type of transponder, known as an Automatic Dependent Surveillance Broadcast, or ADS-B for short, will determine the aircraft's real-time position and velocity by reference to satellites. The fact that the data will be real-time will have a significant impact on separation minimums between aircraft as current radar based systems can take up to 30 seconds to acquire a fix on an aircraft. This time delay manifests itself as a source of error in estimating where an aircraft is at any given moment and requires larger separation between aircraft than is otherwise necessary. This new, more accurate system will allow more aircraft to occupy the same size airspace, helping to ease congestion. This may not effect operations in terminal areas where separation minimums are based largely on wake turbulence factors and the time needed to takeoff or land. However in cruise flight, climb, and decent, smaller separation minimums results in more space to maneuver in the most efficient way possible for the aircraft.

The fuel burn advantages from the ability to maneuver through airspace more freely could be significant. Being able to directly climb to the most efficient altitude for your aircraft instead of the current method of step climbing and then staying at that most efficient cruise altitude for as long as possible before gliding to your final destination using an idle thrust decent is example of a fuel saving maneuver. This maneuver will be possible with NextGen in moderate traffic scenarios. Less time in holding patterns at fuel inefficient, mid-level altitudes will also

be a benefit of NextGen. Finally, and most importantly, point to point routing will be more feasible, cutting fuel burns significantly[45]. Figure 12.1 shows an example of this concept.

Figure 12.1 Actual route versus optimal route between IAD and BOS[45].

The actual route is an example of current routing methods which involve navigating via ground-based navigation aids. The optimal route is a straight line routing between the two airports pictured. With less distance to cover, this point to point routing will also help reduce fuel burn.

Finally, there will be several important safety advantages to the incorporation of the NextGen system. First, air traffic will be displayed for the pilot to see as well as the controller. Figure 12.2 below shows how the ADS-B system will interact with both pilot and controller.

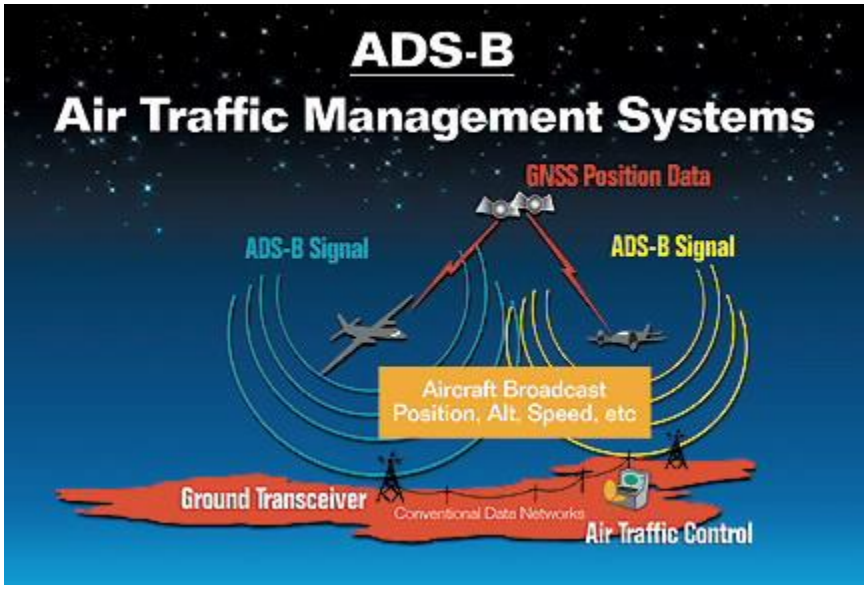

Figure 12.2 ADS-B system of reporting data to pilot and air traffic controller[46].

With both pilot and ground controller both closely interpreting airspace data, the likelihood of a midair collision is reduced and maneuvering through congested airspace will be easier. Next, routine data will be transmitted digitally. This data will include things like simple route changes, course deviations for weather, and turbulence reports. This will free up clogged radio waves for someone who really needs help and will reduce the chances of a pilot not hearing a controller correctly over the radios. Also, weather will be displayed onboard from weather satellites for better situational awareness in poor weather. Finally, air traffic control will be available in areas that lack reliable radar coverage, principally areas over open water[46].

13 Cost

An important factor outlined in the RFP is the cost estimation of the aircraft and how it compares to that of existing aircraft of comparable class. Several key features of the Planeteer's design will affect its cost in a different way than its competitors, namely the use of algae fuel and advanced materials. These change the costs associated not only with flight but all of the subsequent ground and service support systems required as well. The two areas of cost most relevant to these issues are the acquisition cost and operating cost.

13.1 Acquisition Cost

The acquisition cost is defined as the cost of manufacturing plus the profit made on the aircraft. The cost of manufacturing then is the primary driver and provides a good parameter for comparing the aircrafts with the others in its class. Utilizing Roskam's[48] cost analysis methodology, an equation for manufacturing cost is obtained:

$$C_{MAN} = C_{aed_m} + C_{apc_m} + C_{fto_m} + C_{fin_m} \tag{13.1}$$

where C_{aed} is the airframe engineering and design cost, C_{apc} is the production cost, C_{fto} is the flight test operations cost, and C_{fin} is the cost of financing the manufacturing program. Many of these parameters include the costs of detailed items for which no standard list of pricing is given. Certain terms, however, are weighted based on the technical difficulty of the aircraft, and so provide an outline for extrapolating relative costs. For example, the implementation of laminar flow devices will increase the research, development, and production terms by the use of a weighted coefficient determined from its complexity and the inherent costs associated with it. Such a term can increase cost by up to 50% over similar craft with less aggressive use of new technology. Materials are also a significant contributor to manufacturing cost. The planeteer's extensive use of high performance materials such as carbon fiber and titanium will, at current price values, increase its cost. Table 13.1 provides the current costs of a few of these materials compared with more traditional ones.

Table 13.1 Costs of common aircraft materials

Material	Al Alloy 2024-TO	Al Alloy 7075-TO	CFRP	AF1410 Steel	Ti Alloy AMS 4914	Ti-6A-4V Annealed
Cost ($/lb)	1.29	1.25	25.82	5.41	38.43	1.25
Relative Cost (times more expensive)	1	1	20.7	4.3	30.9	1

Titanium is seen to be by far the most expensive material, with carbon fiber reinforced composites the second most. The cost of titanium is driven by its relative abundance on the planet, and thus is unlikely to drop in price. CFRP's however, which have the potential to be extensively used in the construction of the aircraft, are more expensive due to their newness and the complexity involved in their manufacturing. This has the potential to decrease significantly though as composites become more widely used and the techniques for producing them ever more refined. A current cost of the aircraft would be driven up by these prices, however it may not be as substantial a factor by the time it goes into production, and thus minimize the some of the expected higher values in the Planeteer's cost relative to its competitors.

13.2 Operating Cost

The use of algae fuel distinguishes the Planeteer from the other transports in its class. This also provides a significant discrepancy in the cost of operation between it and other planes as well. There are two types of operating cost of significance to this, direct and indirect. Direct operating costs deals with the all of the costs associated with the flight, in particular the price per nautical mile. Table 13.2 provides a quick glance at the comparative energy densities and costs of algae fuel and traditional Jet-A fuel.

Table 13.2 Energy and cost comparisons of Jet-A and Algae fuels

	Energy Denstiy (MJ/kg)	US dollar/ gallon
Jet A Fuel	43.2	~2
Algae Fuel	43	~10

First it is important to note nearly identical energy densities of Jet A and Algae fuel. This makes the comparison of dollar per gallon a direct insight into the operating cost of conventional aircraft and the Planeteer. It is important to note that both of these prices are extremely volatile, and there is no definitive static value. This being said the trend in each is important to look at. Petroleum based fuels such as Jet A are very likely to only continue increasing in price as the cost of drilling and refining oil ever increases. The opposite is said for Algae fuel, and as manufacturing techniques become more refined the price is sure to drop. More recent estimates have put the figure somewhere between 1 and 2 dollars per gallon. The advantage to algae fuel then is its sustainability. The nature of its production does not depend on the limited resources buried in the earth, and so once manufacturing techniques become

optimized there will more than likely be much more stability in price, which will be fixed at a low value. This has enormous potential benefits for the Planeteer as airline companies will be interested in a low, steady operating cost.

Indirect operating costs encompass the other costs associated with the aircraft which are not directly associated with flight, i.e. oil refinement and servicing systems. Again the use of algae fuel distinguishes the Planeteer from more conventional aircraft in this regard. The storage and pumping methods are relatively un-affected due to algae fuels "drop-in" nature, but the manufacturing and production are.

One major concern with the use of biofuels in general is the large amount of land required to produce a meaningful amount of it, and thus the economic as well as social impacts associated with it. The use of more typical biofuels such as those derived from soybeans, sugar cane, and other such crops would require an area half the size of United States to replace all currently used petroleum based fuels with soy biofuels of comparable grade.[49] As population grows and the demand for food continues to increase it is not practical to devote so much land to the production of fuel. Algae fuel however is estimated to have a 30 times greater yield per acre than the other biofuel crops. This translates to an area of 15,000 square miles to replace all petroleum fuel in the U.S., which is roughly equivalent to 2/3 the area of West Virginia. While this is still a significant amount of land, the other benefit of algae fuel is that it may be grown anywhere and does not have to exhaust the arable land which most foods must be grown on. It can be grown in arid, aquatic, or otherwise unusable areas.

There are tremendous benefits to the use of algae fuels. The major obstacle to their use however, is their relatively difficult extraction and refinement process. The extent that algae fuels will be grown and refined greatly affects this indirect operating cost. If there is a large market for algae fuel in the future then its manufacturing and production costs will surely be decreased. In this case the Planeteer's use of such algae fuel will be very beneficial from an environmental as well as a cost perspective.

14 Conclusion

CP Aeronautics began designing the Planeteer by comparing similar 175 seat commercial airliners currently in service. This led to three initial designs, the conventional wing, blended wing body, and strut-braced wing. Through careful analysis the strut-braced design was chosen for the Planeteer. The design was then sized to the specifications set in the RFP.

The Planeteer uses a combination of new engine, wing, and materials technology to meet or exceed all of the RFP requirements. The strut-braced wing concept allows for a higher lift-to-drag ratio which results in more efficient flying. A 49% improvement in L/D over the Boeing 737-800 was achieved. The Planeteer seats 175 passengers in a single class with comfortable seat dimensions. The plane's maximum range is 4,800 nm miles instead of the RFP's requirement of 3,500 nm. The Planeteer's takeoff length is only 4,800 ft, nearly half of that required by the RFP. The wing and engines allow the plane to cruise at 40,000 ft with an absolute ceiling of 41,000 ft. The wing also allows a landing speed of 135 knots. The Planeteer will be certifiable to appropriate FARs for entry into service by 2020. Overall, the Planeteer meets and in most cases surpasses all the requirements provided by the 2010 AIAA RFP.

15 References

[1] Lewis, M.J., "Military aviation goes green," *Aerospace America*, September, 2009, pp. 24-31.

[2] "CSeries Family," Bombardier Aerospace, Montreal, Canada, 2008, http://www.bombardier.com/en/aerospace/products/commercial-aircraft/cseries?docID=0901260d800091e6 [retrieved 28 January 2010].

[3] "737 Airplane Characteristics for Airport Planning," Boeing Commercial Airplanes, D6-58325-6, Seattle, WA, October 2005.

[4] *Jane's All the World's Aircraft 2009-2010*. Jane's Publishing Co, New York, 2009.

[5] R.E. Liebeck,"Design of the Blended Wing Body Subsonic Transport", *Journal of Aircraft* 2004, 0021-8669, vol.41, no.1 (10-25), doi: 10.2514/1.9084

[6] S. Cho, C. Bil, J. Bayandor, "Structural Design and Analysis of a BWB Military Cargo Transport Fuselage", RMIT University, AIAA-2008-165 , 46th AIAA Aerospace Sciences Meeting and Exhibit, Reno, Nevada, Jan. 7-10, 2008.

[7] Mason, W. H., "Why Airplanes Look Like They Do," AOE 4065-4066 Design (Aircraft), Virginia Tech, Virginia, August 2009. [http://www.aoe.vt.edu/~mason/Mason_f/SD1L3.pdf. Accessed 11/16/09.]

[8] Raymer, Daniel P., *Aircraft Design: A Conceptual Approach. 4th ed*, AIAA, Reston, VA, 2006.

[9] "Civil Turbojet/Turbofan," [online database], http://jet-engine.net/civtfspec.html [retrieved 1 December 2009].

[10] "737 Airplane Characteristics for Airport Planning," 737-BBJ Document D6-58325-6, http://www.boeing.com/commercial/airports/acaps/737.pdf, [retrieved 1 December 2009].

[11] "All About the A320 Family Technical Appendices," http://www.airbus.com/fileadmin/media_gallery/files/other/media_object_file_2009-All-About-A320Family-Tech-appendices.pdf, [retrieved 1 December 2009]

[12] Harris, Charles D., "NASA Supercritical Airfoils," NASA TP 2969, 1990.

[13] Green, John E., "Laminar Flow Control-Back to the Future?," *38th Fluid Dynamics Conference and Exhibit*, Seattle, Washington, June 2008, AIAA 2008-3738.

[14] Selig, Michael, "UIUC Airfoil Coordinates Database," UIUC Applied Aerodynamics Group, 1995 to present. [http://www.ae.illinois.edu/m-selig/ads/coord_database.html]

[15] Mason, William H., "The connection between the critical Mach number and the drag divergence Mach number, and a Poor Man's way of estimating the drag rise curve," 2009.

[16] "PurePower PW1000G," Pratt & Whitney, http://www.pw.utc.com/vgn-ext-templating/v/index.jsp?vgnextoid=59ab4d845c37a110VgnVCM100000c45a529fRCRD [retrieved 14 April 2010].

[17] Butterworth-Hayes, P., "Open Rotor Research Revs Up," *Aerospace America*, March, 2010, pp. 38-42.

[18] "The PW-1000G geared turbofan engine," Volvo Aero, http:// www.volvoaero.com/ volvoaero /global /en-gb/ products/ Engine%20components/ commercial_ engines/ Pages/ pw1000G.aspx [retrieved 14 April 2010].

[19] "Lettin' it all hang out," Student Engineer Help, June 20 2009, http:// studentengineerhelp.com/ 2009/ 06/ 20/ lettin-it-all-hang-out/ [retrieved 14 April 2010].

[20]Roskam, Dr. Jan. "Part V: Component Weight Estimation." *Airplane Design*. Lawrence, Kansas: DARcorporation, 2003.

[21]Naghshineh-Pour, Amir H. "Structural Optimization and Design of a Strut-Braced Wing Aircraft." MS Thesis, Aerospace & Ocean Engineering. Blacksburg, Virginia, 1998.

[22]van Hoek, Maarten. "Design of a Strut-Braced Wing Truss Support System." Aerospace & Ocean Engineering. Blacksburg, Virginia, 2007.

[23]Johnson, Dr. Eric. "AOE 3124 Aerospace Structures." Aerospace & Ocean Engineering. Blacskburg, Virginia, 2008.

[24] Anderson, John D. Jr. "Elements of Aircraft Performance." *Introduction to Flight.* 5th edition. McGraw-Hill, New York, 2005.

[25] Gundlach, John F. IV, "Multidisciplinary Design Optimization and Industry Review of a 2010 Strut-Braced Wing Transonic Transport," Masters Thesis, Department of Aerospace and Ocean Engineering, Virginia Tech, Blacksburg, VA, 1999.

[26] Morrow, Mike, "Aircraft Mission Performance Evaluation: Part of the Virginia Tech Aircraft Design Software Series," Aerospace and Ocean Engineering Department, Virginia Tech, Blacksburg, VA, 2002 (unpublished).

[27] *CES EduPack Selector Version 4.8.0*. CD-ROM. Granta Design Limited, 2008.

[28]Roskam, Dr. Jan. "Part VII: Determination of Stability, Control and Performance Characteristics: FAR and Military Requirements." *Airplane Design*. Lawrence, Kansas: DARcorporation, 2003.

[29] "LDstab sizing program." 20 February 2009 <http://www.aoe.vt.edu/~mason/Mason_f/MRsoft.html#Nicolai>.

[30] "Tornado VLM." 20 February 2009 <http://www.aoe.vt.edu/~mason/Mason_f/MRsoft.html#Nicolai>.

[31] B. Etkin and L. D. Reid. *Dynamics of Flight: Stability and Control*. John Wiley and Sons, New York, NY, third edition, 1996.

[32] Wallace, J.,"Boeing's high tech 787 flight deck", seattlepi, http://blog.seattlepi.com/aerospace/archives/115988.asp [retrieved 14 April 2010].

[33] "Boeing 737-800 Seating Plans", SeatPlans.com, http:// www.seatplans.com/ airlines/ Ryanair/ seatplan-classes/ B737-800-8-Economy-56 [retrieved 14 April 2010].

[34] Yoon, J., "Aircraft Lights & Beacons", aerospaceweb.org, 26 February 2006, http:// www.aerospaceweb.org/ question/ electronics/ q0263.shtml [retrieved 14 April 2010].

[35] Sloan, J., "787 integrates new composite wing deicing system," *High-Performance Composites*, published online 30 Dec. 2008; January 2009, http:// www.compositesworld.com/ articles/ 787-integrates -new-composite -wing-deicing -system [retrieved 14 April 2010].

[36] "Airport Design," Federal Aviation Administration, Advisory Circular (AC) 150/5300-13 Change 10, U.S. Department of Transportation, 29 September 2006.

[37] Williams, J., "Talking Algae Biofuels with Solazyme and Aquaflow," Celsias, March 2009, http://www.celsias.com/article/talking-algae-biofuels-solazyme-and-aquaflow/ [retrieved 20 October 2009].

[38] Danigole, M. S., "Biofuels: An Alternative to U.S. Air Force Petroleum Fuel Dependency," USAF, February 2007.

[39] Graham, I., "Air Force Scientists Test, Develop Bio Jet Fuels," af.mil, March 2010. [http://www.af.mil/news/story.asp?id=123197415. Accessed 4/15/10.]

[40] Stone, J., "Air New Zealand's Biofuel Flight Cuts Emissions," gas2.0, June 2009, [http://gas2.org/2009/06/01/air-new-zealands-biofuel-flight-cuts-emissions-by-65/. Accessed 4/15/10.]

[41] O'Connell, D., "KLM Biofuel Flight Fuels Hopes for Green Airlines," Business Times Online, November 2009. [http://business.timesonline.co.uk/tol/business/industry_sectors/transport/article6936255.ece. Accessed 4/15/10.]

[42] "Continental Airlines Reports That the Biofuel Blend on its Test Flight Performed Better than Traditional Jet Fuel," Green Air Online, June 2009. [http://www.greenaironline.com/news.php?viewStory=505. Accessed 4/15/10.]

[43] Warwick, G., "EADS Backs Algae as Future Biofuel," Aviation Week, March 2010. [http://www.aviationweek.com/aw/generic/story_generic.jsp?channel=aviationdaily&id=news/avd/2010/03/19/01.xml. Accessed 4/15/10.]

[44] "NextGen 2018," FAA, 27 February 2009, http:// www.faa.gov/ about/ initiatives/ nextgen/ 2018/ [retrieved 14 April 2010].

[45] "Peterson, B. S., "End of Flight Delays? FAA's GPS Fix Could Bust Sky Gridlock," *Popular Mechanics*, http://www.popularmechanics.com/science/space/4219569 [retrieved 14 April 2010].

[46] "NextGen Fact Sheet," FAA, Washington, DC, February 2007, http://www.faa.gov/news/fact_sheets/news_story.cfm?newsid=8145 [retrieved 20 October 2009].

[47] Loftin, Laurence K., Jr, "Subsonic Aircraft: Evolution and the Matching of Size to Performance," NASA, RP-1060, 1980.

[48] Roskam, D., "Part VIII: Airplane Cost Estimation: Design, Development, Manufacturing and Operating," *Airplane Design*, edited by D. Roskam, Roskam Aviation and Engineering Corporation, The University of Kansas, 1990.

[49] Hartman, E., "A Promising Oil Alternative: Algae Energy," The Washington Post, January 2008. [http://www.washingtonpost.com/wp-dyn/content/article/2008/01/03/AR20080103039 07.html. Accessed 4/27/2010.]

[50] Sinnett, M., "787 No-Bleed Systems: Saving Fuel and Enhancing Operational Efficiencies," AERO Magazine, Q4 2007, http://www.boeing.com/ commercial/aeromagazine/ articles/qtr_4_07/ article_02_1.html [retrieved 5 May 2010].

[51] Mason, William, "High-Lift Aerodynamics," *Configuration Aerodynamics* [online] Blacksburg, VA, 5 April 2006, http://www.aoe.vt.edu/~mason/Mason_f/ConfigAero.html [retrieved 6 May 2010].

[52] Murman, E.M., Bailey, F.R., and Johnson, M.L., "TSFOIL – A Computer Code for Two-Dimensional Transonic Calculations, Including Wind-Tunnel Wall Effects and Wave Drag Evaluation," NASA SP-347, March 1975.

[53] Drela, Mark, "XFoil," Massachusetts Institute of Technology, Cambridge, MA, November 2007.

[54] Mason, William, "Friction – Skin Friction and Form Drag Program," Department of Aerospace and Ocean Engineering, Virginia Tech, Blacksburg, VA, January, 2006.